博士論文

論文題目 **The end-Guadalupian (Permian) mass extinction and relevant environmental changes in the superocean Panthalassa: litho-, bio-, and chemostratigraphy of accreted paleo-atoll limestones in Japan**
（超海洋パンサラサにおけるガダルピアン世（ペルム紀）末の大量絶滅と環境変動：日本に付加した古礁石灰岩の岩相・生・化学層序）

氏　名　　小 福 田　　大 輔

Abstract

The biggest mass extinction of the Phanerozoic occurred at the end of the Paleozoic, ca. 252 million years ago (Ma); in fact in two steps, i.e. first at the boundary between the Guadalupian (Middle Permian) and Lopingian (Late Permian) (ca. 260 Ma), and second at the boundary between the Permian and the Triassic (ca. 252 Ma). The Guadalupian-Lopingian boundary (G-LB) event is more significant than that of the Permian-Triassic boundary, because this event marked the first large decline of the long-lasting Paleozoic fauna. Despite over 100 year-long previous studies about the end-Paleozoic extinction event, the main cause of the extinction has not yet been identified. This study analyzed litho-, bio-, and chemostratigraphy of the Middle-Upper Permian limestone in Japan, in order to identify the nature of extinction-related environmental changes.

The Capitanian (upper Guadalupian) to Wuchiapingian (lower Lopingian) shallow-marine limestones at Akasaka and Ishiyama in central Japan record unique aspects of the extinction-related G-LB interval, because they preserve extremely rare environmental records of mid-superocean. The ca. 140 m-thick Akasaka Limestone consists of the Capitanian black bioclastic limestone (Unit B; 112 m) and the overlying Wuchiapingian light gray dolomitic limestone (Unit W; 21 m), with a black/white striped limestone (Unit S; 9 m) between them. The G-LB horizon is assigned at the base of Unit W, on the basis of the first occurrence of the Wuchiapingian fusulines.

The Capitanian Unit B and the Wuchiapingian Unit W were deposited mostly in the subtidal zone in a lagoon setting of an atoll, whereas the intervened Unit S and the lowermost Unit W were in the intertidal zone. A hiatus with a remarkable erosional feature was newly identified at the top of Unit S. This indicates that the sea-level dropped significantly around the G-LB to have exposed the top of the atoll complex above the sea-level. Almost the same depositional record was confirmed in the Ishiyama Limestone located ca. 10 km to the north of Akasaka.

The extinction of large-tested fusuline (*Yabeina*) and large bivalves (Alatoconchidae) occurred in the upper part of Unit B, and the overlying 20 m-thick limestone (the uppermost Unit B and Unit S) below the hiatus represents a unique barren interval. The upper half of the barren interval is more depleted in fossils than the lower half, and this likely represents a duration of the severest environmental stress(es) for the shallow-marine protists/animals on the mid-oceanic paleo-atoll complex. Small-tested

fusulines re-appeared at the base of Unit W immediately above the hiatus. These facts prove that the elimination of shallow-marine biota occurred during the Capitanian shallowing of Akasaka paleo-atoll before the subaerial exposure/erosion across the G-LB. The overall shallowing and the development of a clear hiatus at the top of a mid-oceanic seamount indicates that a remarkable sea-level drop had occurred globally during the latest Capitanian in accordance with the contemporary sea-level curve based on continental shelf records. This further suggests that a cool climate likely has appeared even in the low-latitude domains in Panthalassa to cause the decline of the Middle Permian shallow-water protists/animals that were adapted to warmer seawaters. The Wuchiapingian biota first appeared immediately after this erosional episode, i.e., during the onset of warming after the G-LB.

In order to access the extinction-relevant changes in mid-oceanic surface seawater, this study analyzed carbon and strontium isotope ratios of bulk carbonate. As to inorganic carbon isotope ratio of seawater ($\delta^{13}C_{carb}$), very high value (> +5.0 ‰) was detected in the upper Capitanian, and dropped across the G-LB. This pattern suggests stable high-productivity by enhanced oceanic circulation in the Capitanian and following rapid drop across the G-LB. $^{87}Sr/^{86}Sr$ was extremely low (<0.7070) throughout the Capitanian and sharply rose up to 0.7073 across the G-LB, indicating the long-term suppression of continental flux into the superocean, and following increase. This pattern can be explained in terms of the expansion of continental glacier in the Capitanian and following shrink across the G-LB. These isotopic patterns are concordant with the Capitanian global cooling and following warming after the G-LB suggested by the litho- and biostratigraphy.

On the basis of these new results, I conclude that the end-Capitanian mass extinction event was caused likely by the global cooling during the late Guadalupian. The faunal recovery in the Late Permian apparently occurred during the global warming after the G-LB.

Contents

1. Introduction

The largest mass extinction event of the Phanerozoic (e.g. Sepkoski, 1984; Erwin, 2006; Bottjer et al., 2008; Alroy, 2010) (Fig. 1.1) occurred in two steps at the end of Paleozoic; i.e., first immediately before the Middle-Late Permian boundary (Guadalupian-Lopingian boundary; G-LB; 260 Ma), and second at the Permian-Triassic boundary (P-TB; 252 Ma) (e.g. Jin et al., 1994; Stanley and Yang, 1994; Bambach, 2006) (Fig. 1.2). The diversity decline around the G-LB was recently revealed to have been not so rapid as previously believed (Clapham et al., 2009) and the main extinction occurred within the late Guadalupian clearly before the biostratigraphically-defined G-LB (Isozaki and Ota, 2001; Ota and Isozaki, 2006; Retallack et al., 2006). Nonetheless, the late Guadalupian event appears significant, somehow more important than the P-TB event, because the overall long-term high biodiversity of the Permian shallow marine fauna dropped drastically for the first time prior to the G-LB (e.g. Isozaki, 2009; Groves and Wang, 2013).

In addition to the extinction, several other unique geologic events of global scale occurred in the Capitanian (Late Guadalupian); e.g. sea-level dropped to the Phanerozoic lowest around the G-LB, global oceanic anoxia started in the Capitanian, $\delta^{13}C_{carb}$ of seawater started volatile fluctuation and $^{87}Sr/^{86}Sr$ of seawater hit the minimum of the Phanerozoic, as summarized by Isozaki (2009) (Fig. 1.3). It is also noteworthy that a major pattern change in geomagnetic polarity (Illawara Reversal) occurred slightly earlier than the onset of the above-mentioned isotopic changes (Isozaki, 2007, 2009). All of these global phenomena are exceptionally rare in the Phanerozoic, but unique to the terminal interval of the Middle Permian, i.e., the first critical timing for the Paleozoic life. All these geologically rare phenomena occurred uniquely during the late Middle Permian not likely by accident but probably in intimate cause-effect relationships among each other, although details are still in discussion (Isozaki, 2009). As to the cause of the G-LB extinction, various candidates were proposed, such as global regression (Jin et al., 1994), massive eruption of Emeishan flood basalt in South China (Zhou et al., 2002; Wignall et al., 2009), massive emission of methane (Retallack et al., 2006), global cooling (Isozaki et al., 2007b); however, the ultimate cause of the G-LB extinction event has not yet been clarified.

Most of previous studies on the G-LB focused on the fossiliferous strata deposited on

the continental shelves around Paleo-Tethys that formed a large embayment of the supercontinent Pangea. Restricted information solely from the Palaeo-Tethyan domain, however, may not represent the entire record of global environmental changes on the Earth's surface. From a contrasting different viewpoint, Isozaki and Ota (2001) and Ota and Isozaki (2006) clarified for the first time the mid-Panthalassa records from G-LB paleo-atoll limestone originally deposited in the middle of the superocean Panthalassa. As well as the modern world, oceans occupied nearly 70 % of the Earth's surface then either (Fig. 1.5); however those seafloors have been completely lost by the successive subduction processes. Within ancient accretionary complex exposed on land, however, remnants of such lost ocean floors are preserved.

In Southwest Japan, the late Paleozoic to Mesozoic accretionary complexes include numerous exotic blocks of Carboniferous and Permian limestone, which were derived from mid-oceanic atoll complexes developed primarily on the top of seamounts, and were secondarily transported/accreted to the Asian continental margins including Japan (e.g. Kanmera and Nishi, 1983; Sano, 1988; Sano and Kanmera, 1988; Isozaki et al., 1990; Isozaki, 1997) (Fig. 1.6). The Permian Iwato Formation of the Jurassic accretionary complex in Kyushu (Fig. 1.7) is one of these accreted paleo-atoll limestone (Ota and Isozaki, 2006; Kasuya et al., 2012). The paleomagnetic analysis clarified that this Permian limestone was deposited in the mid-oceanic, low-latitude area (12°) in the southern hemisphere (Kirschvink and Isozaki, 2007).

In particular, the Akasaka Limestone in central Japan represents another major exotic block in the Jurassic accretionary complex of the Mino-Tanba belt (Fig. 1.7). Since the Akasaka Limestone yielded numerous well-preserved megafossils, such as large gastropods and bivalves, biostratigraphic studies have been carried out since the second last century (e.g. Gümbel, 1874; Schwager, 1883; Yabe, 1902; Karpinsky, 1908; Depart, 1914; Hayasaka, 1925; Ozawa, 1927). The overall stratigraphy of the Akasaka Limestone was revealed by Akasaka Research Group (1956), Sakagami (1980), Ozawa and Nishiwaki (1992), Zaw Win (1999), Isozaki and Ota (2001), Ota and Isozaki (2006), and Kobayashi (2011). As to the G-LB interval, Ota and Isozaki (2006) first documented a unique lithofacies change across the G-LB with respect to the end-Guadalupian extinction of large-tested fusulines, thus the Akasaka Limestone provide the best target for the G-LB study.

The mid-oceanic paleo-atoll limestones potentially recorded secular change in

seawater composition, including some isotope signatures, e.g. carbon and strontium. As to the carbon isotope ($\delta^{13}C_{carb}$), there are negative shifts both P-TB and G-LB (e.g. Baud et al., 1989; Holser et al., 1989; Musashi et al., 2001; Wang et al., 2004; Korte et al., 2005). In addition, unique high positive $\delta^{13}C_{carb}$ values (+5 to +6 ‰) were detected in the Capitanian in the mid-superocean (Isozaki et al., 2007a, b). Such high positive values were rare in the Phanerozoic except for the several events in the Paleozoic (e.g. Veizer et al., 1999; Saltzman, 2005). This episode in the Capitanian was named "Kamura event" emphasizing its significance of global cooling and relevant extinction of tropical trio (rugose coral, large fusulines, giant bivalves).

On the other hand, strontium isotope ratio ($^{87}Sr/^{86}Sr$) of seawater has changed significantly through time. One of the unique features is the "Capitanian minimum" that occurred during the Middle-Late Guadalupian to mark the lowest $^{87}Sr/^{86}Sr$ ratio, ca. 0.7068 (Veizer et al., 1999; McArthur et al., 2012). Ever since the Cambrian, $^{87}Sr/^{86}Sr$ ratio of seawater had decreased throughout Paleozoic with minor fluctuations. After the Capitanian minimum, abrupt increase of $^{87}Sr/^{86}Sr$ ratio occurred to the Middle Triassic, with the most rapid rate in the Phanerozoic (Korte et al., 2006; McArthur et al., 2012). The cause of this long-term change has not yet been identified, although some possible causal links were proposed, such as changes in global tectonics, sea-level, climate, weathering rate and diagenetic processes (e.g. Veizer, 1989; Derry and France-Lenard, 1997; Korte et al., 2003; Banner, 2004).

Previous studies have not documented high-resolution lithostratigraphy immediately below and above the G-LB and relevant pattern of biotic changes. For example, as to the isotope studies, high $\delta^{13}C_{carb}$ Kamura event has not been detected from one continuous section, and the detailed timing of onset and end of $^{87}Sr/^{86}Sr$ Capitanian minimum has not yet been known. In addition, the causal relationship between biotic change and changes in seawater chemistry ($\delta^{13}C_{carb}$, $^{87}Sr/^{86}Sr$) has been unknown. Therefore, this study analyzed details of litho-, bio-, and isotope stratigraphy of the G-LB interval together with the relevant facies change in the Akasaka and Ishiyama limestones, and discusses their geological implications to G-LB extinction.

I studied the lithostratigraphy of the Permian paleo-atoll limestone in the quarries at Akasaka and Ishiyama in central Japan (Fig. 1.7). The G-LB section at Akasaka is less deformed/metamorphosed and the thickness of the coeval interval is greater than the Iwato Fm in Kyushu. Recent active development at quarries in Akasaka (Kawai Lime

Co. and Mitsuboshi Mining Co.) exposed extensive/continuous outcrops of the G-LB interval (Fig. 3.3), giving an opportunity for further study. In addition, the same G-LB interval was exposed in another quarry at Ishiyama (Osaka Mitsubishi Co.) located ca. 10 km to the north of Akasaka (Fig. 3.1). For recovering fresh rock samples, in particular, I conducted two scientific drillings in the properties of Kawai Lime Co. and Mitsuboshi Mining Co. in Akasaka, and another in the properties of Kawai Lime Co. and Osaka Mitsubishi Lime Co.

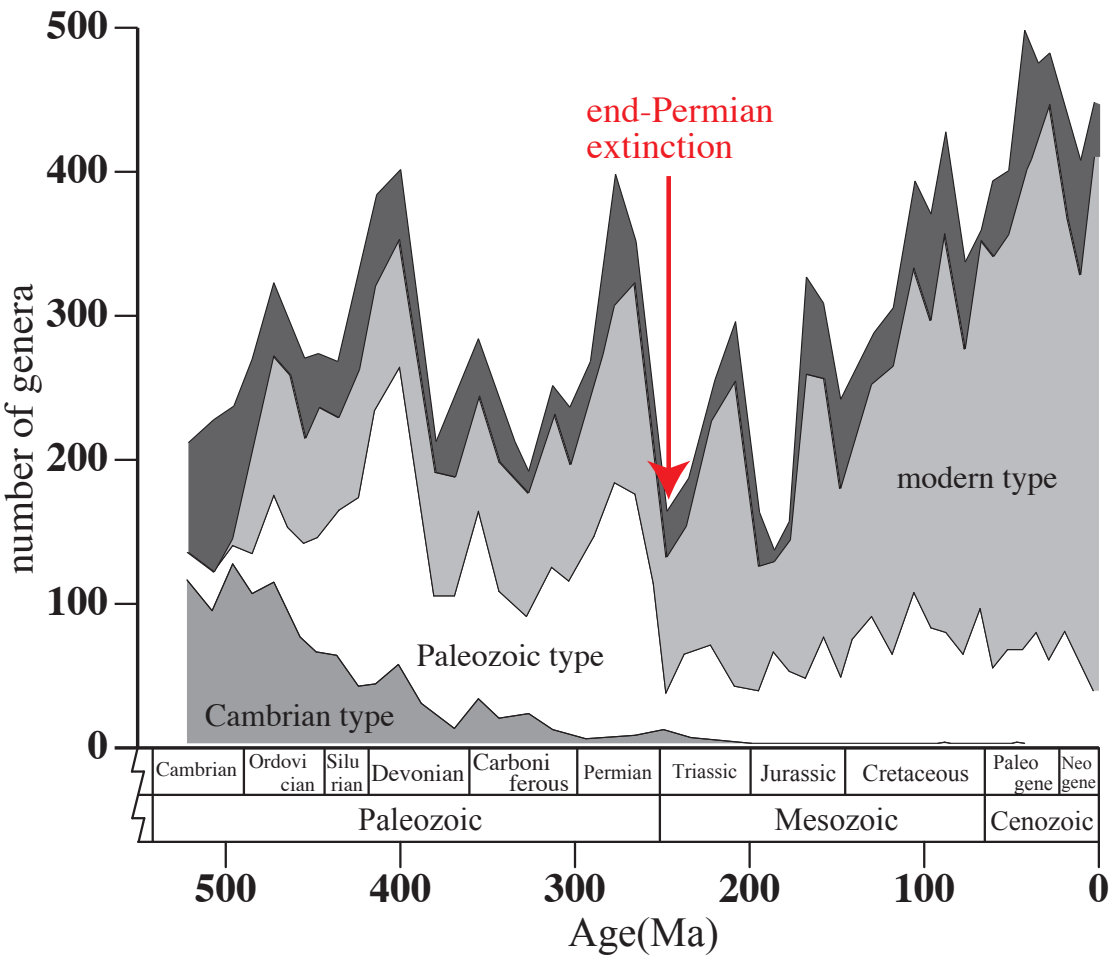

Fig. 1.1. The biodiversity change in the Phanerozoic (modified from Alroy, 2010). The biodiversity drop was the largest at the Permian-Triassic boundary.

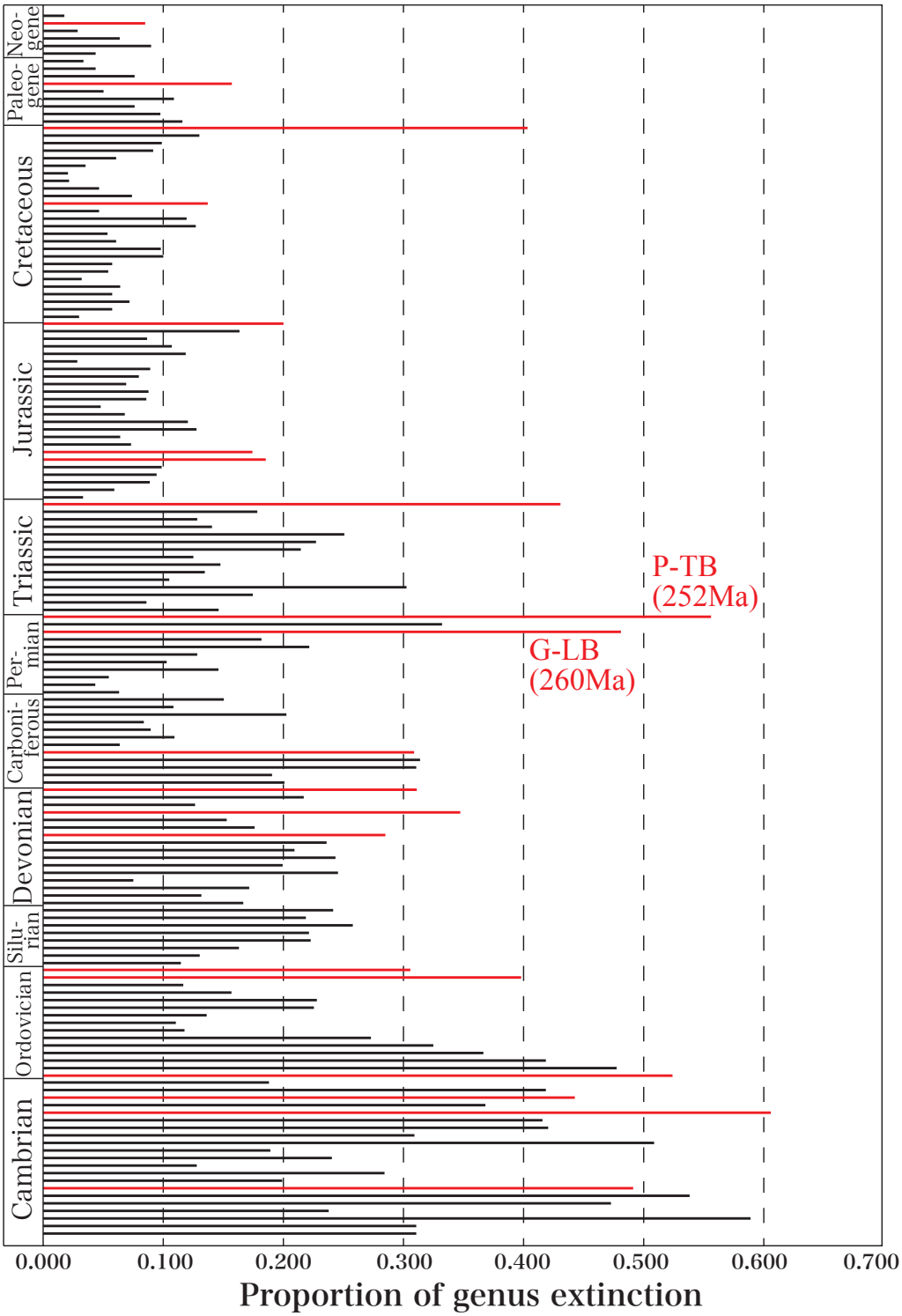

Fig. 1.2. The proportion of genus extinction in the Phanerozoic (modified from Bambach, 2006). Red bars represent mass extinction. Note that the Permian high biodiversity dropped for the first time at the G-LB, not at the P-TB.

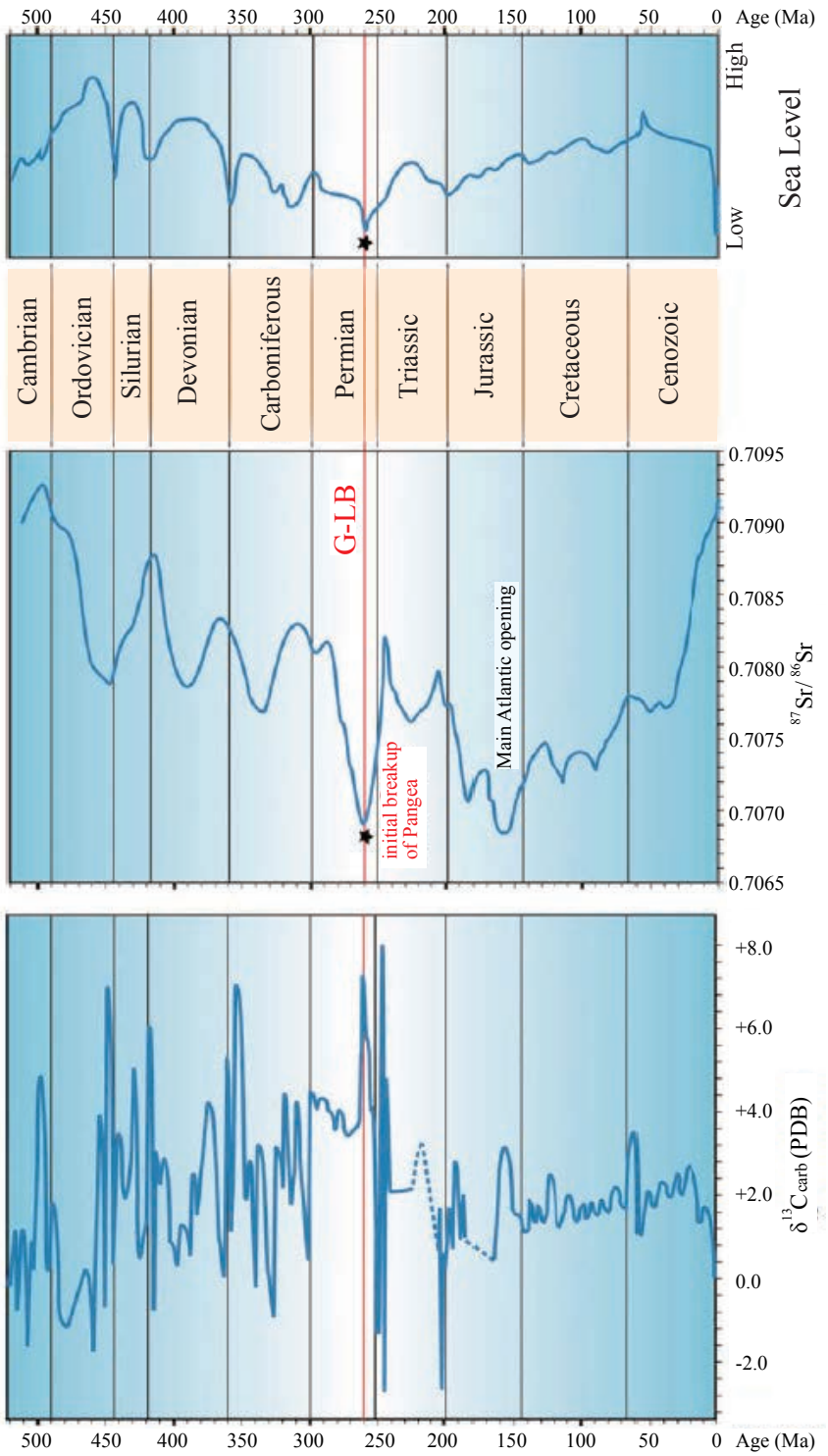

Fig. 1.3. Compilation of $\delta^{13}C_{carb}$ (lower), $^{87}Sr/^{86}Sr$ of seawater (middle) and global sea-level (upper) in the Phanerozoic (Isozaki, 2009). Secular changes such as onset of volatile $\delta^{13}C_{carb}$ fluctuation, $^{87}Sr/^{86}Sr$ minimum and lowest sea-level occurred not at the P-T boundary, but at the G-L boundary.

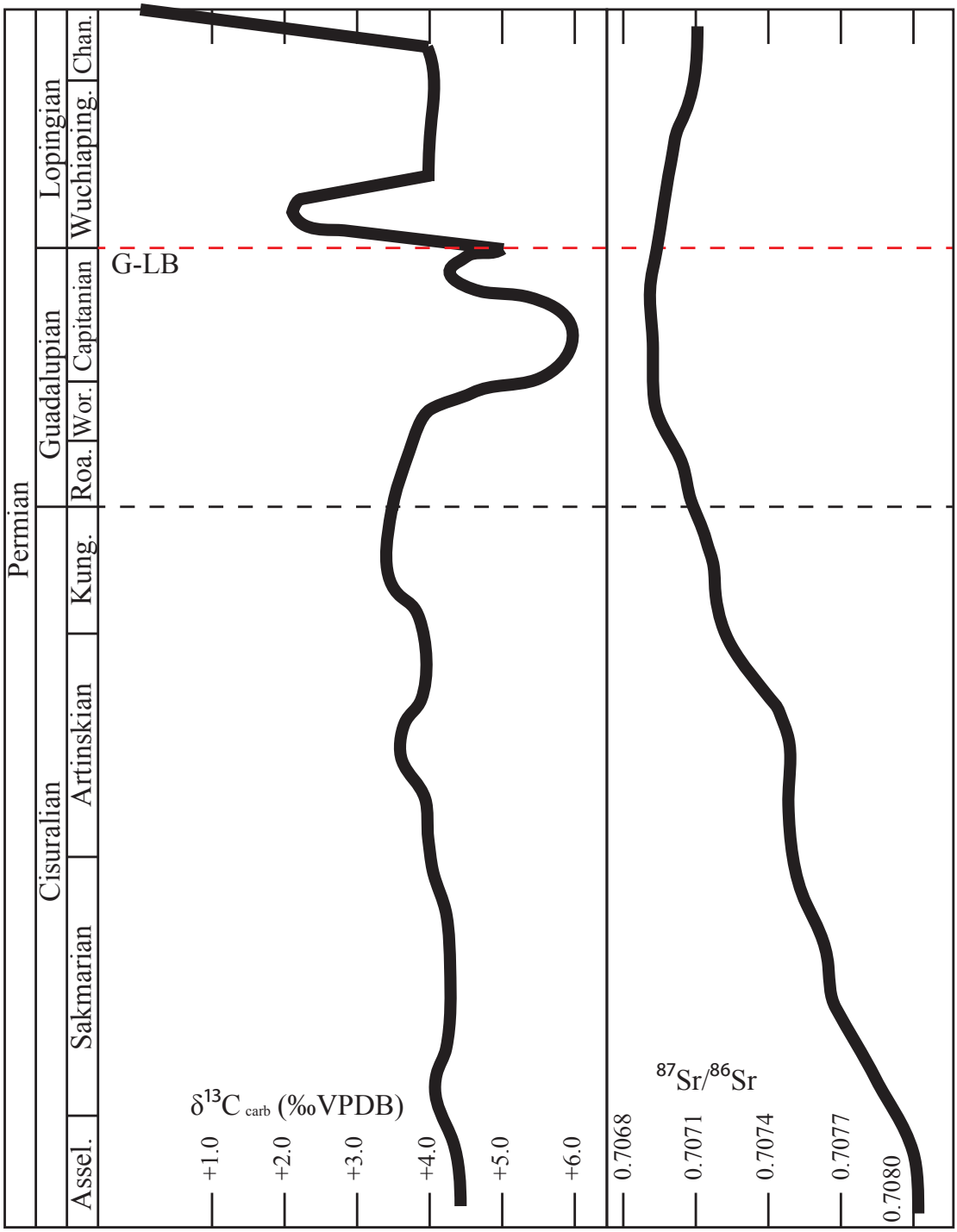

Fig. 1.4. $\delta^{13}C_{carb}$ (left) and $^{87}Sr/^{86}Sr$ of seawater (right) in the Permian (modified from Korte et al., 2005; 2006, Isozaki et al., 2011). $\delta^{13}C_{carb}$ was very high (>5 ‰) and $^{87}Sr/^{86}Sr$ was low (<0.7070) in the Capitanian, but across the G-LB, $\delta^{13}C_{carb}$ sharply dropped, and $^{87}Sr/^{86}Sr$ increased.

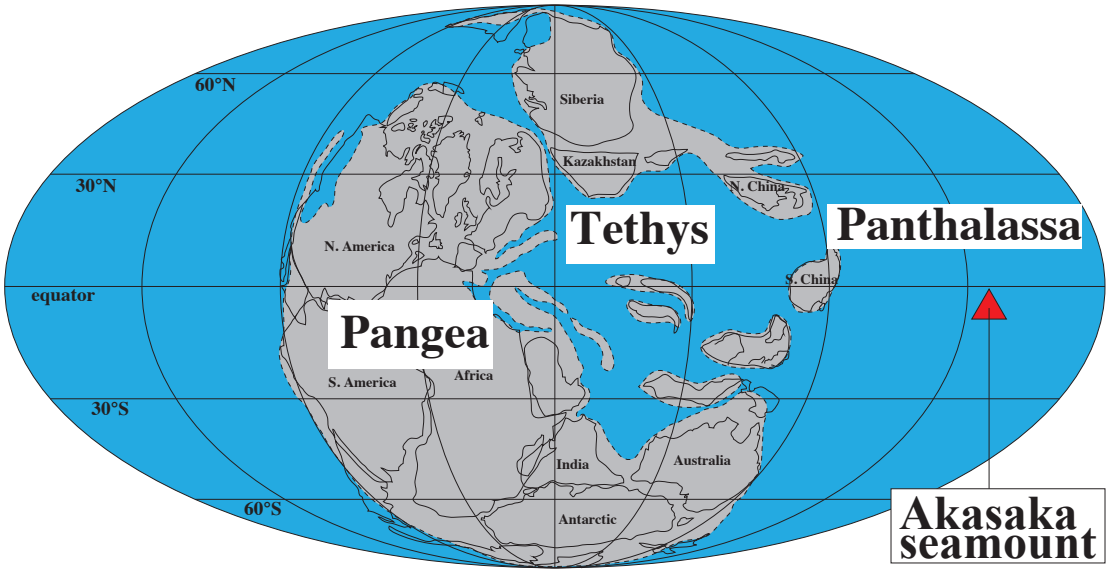

Fig. 1.5. Paleogeography around the G-LB. Note that Akasaka seamount was placed in the low-latitude mid-Panthalassa (modified from Scotese and Langford, 1995).

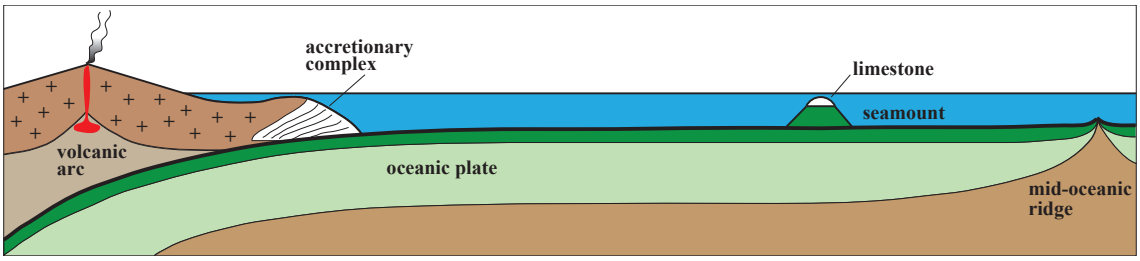

Fig. 1.6. A simplified diagram of a ridge-subduction system showing the tectono-sedimentary setting of the Permian paleo-atoll complex; from the primary deposition on a mid-oceanic seamount to the secondary accretion at a trench (modified from Kani et al., 2013).

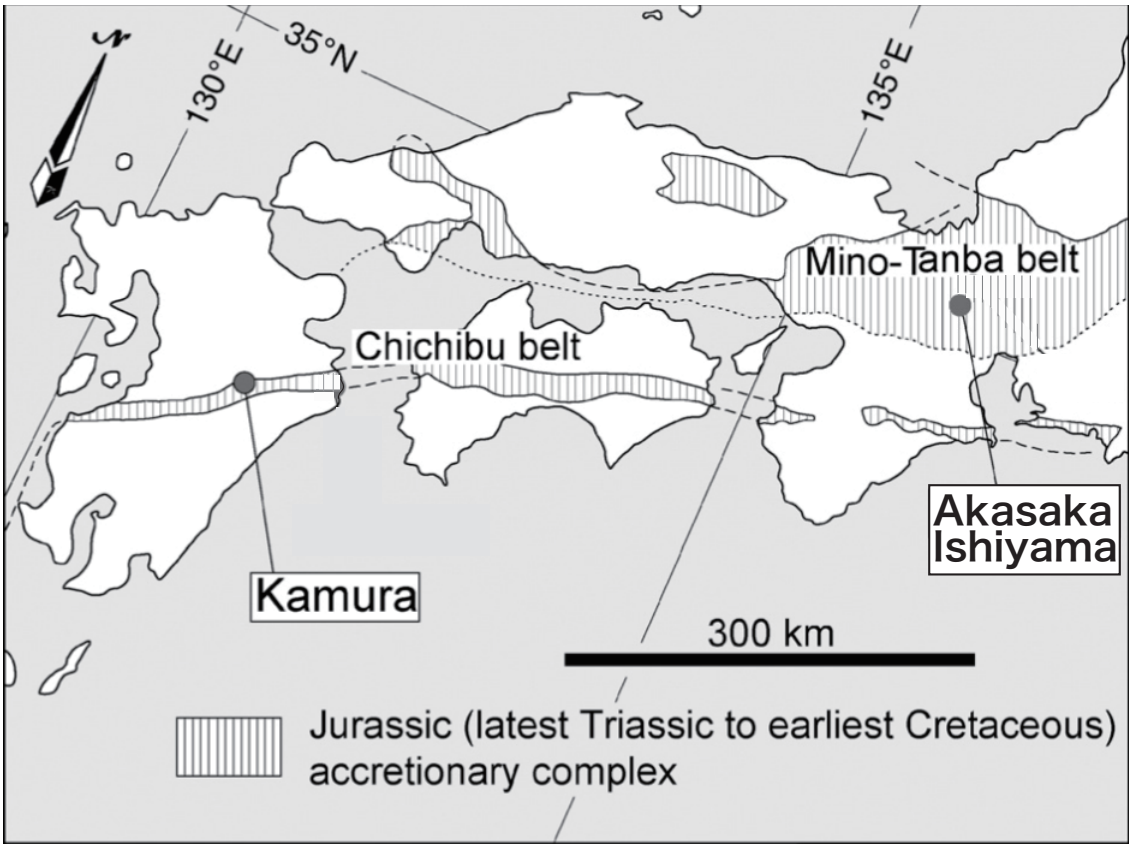

Fig. 1.7. Localities of the Akasaka-Ishiyama area in the Mino-Tanba belt, central Japan, and the relevant Kamura area in the Chichibu belt, Kyushu (modified from Ota and Isozaki, 2006).

2. Historical review of studies on Permian paleo-atoll limestones

The research history of the Permian paleo-seamount can be divided into 3 stages; 1) the 1980s, 2) the 1990s, and 3) the post-2000.

1) In the early 1980s, Kanmera and Nishi (1983) first recognized that exotic blocks of Carboniferous to Permian limestone in the Permian accretionary complex (Akiyoshi belt) in Japan was derived from a paleo-atoll complex originally deposited on the top of a paleo-seamount in the mid-superocean (Kanmera and Nishi, 1983; Sano and Kanmera, 1988). Sano (1988) described another mid-oceanic Permian limestone in the Jurassic accretionary complex (Mino belt), central Japan.

2) In the 1990s, Koike (1996) was the first in the world to recognize the P-TB horizon in such and accreted mid-oceanic limestone by conodont biostratigraphy in Kyushu and Shikoku, southwest Japan. On the basis of this biostratigraphic assignment, Sano and Nakashima (1997) analyzed the unique lithofacies of the P-TB interval in the former example.

3) In the 21st century, studies on paleo-atoll limestone entered a new stage. Isozaki and Ota (2001) for the first time recognized the G-LB in the Kamura and Akasaka limestones, and Ota and Isozaki (2006) documented more details of fusuline biostratigraphy. On the basis of these biostratigraphic analyses around the G-LB, various studies relevant to the G-LB extinction started afterwards.

Isozaki (2006) reported extremely bizarre giant bivalve Alatoconchidae and speculated that the extinction of tropical trio (rugose coral, large fusuline, giant bivalve) was significantly related to global cooling (Isozaki and Aljinovic, 2009). Analyses of carbon isotope stratigraphy were performed by Isozaki et al. (2007a, b) to clarify an extremely high $\delta^{13}C_{carb}$ (> +5 ‰) interval in the Capitanian (Kamura event) with a subsequent sharp drop across the G-LB. As to the strontium isotope stratigraphy, Kani et al. (2008) detected "Capitanian minimum", the lowest $^{87}Sr/^{86}Sr$ ratio (<0.7070) in the Phanerozoic for the first time from mid-Panthalassa, and Kani et al. (2013) further demonstrated the continuity of the low $^{87}Sr/^{86}Sr$ minimum throughout the most of the Capitanian.

The Permian paleo-atoll limestones are regarded to have deposited originally in the low-latitude as indicated by the occurrence of the tropical fauna. In addition,

Kirschvink and Isozaki (2007), for the first time, conducted paleomagnetic analysis and determined the paleo-latitude for deposition at 12° in the southern hemisphere for the Kamura Limestone. By checking the characteristics of the fusuline assemblage, Kasuya et al. (2012) speculated that paleo-seamount might have trespassed a boundary between two biogeographic provinces within the superocean.

All of these results were obtained solely from Japan, and no such attempts were made in the rest of the world. Permian seafloor is totally gone due to plate subduction, thus these results from paleo-atoll limestones can provide one and only data for the Permian mid-superocean. In the future, this kind of approach will be likely applied in much older examples of paleo-atoll limestones in the world.

3. Geologic setting

The two studied areas, Akasaka and Ishiyama, are located in southern part of the Gifu prefecture, ca. 30-40 km to the north of Nagoya city in central Japan (Fig. 3.1). Both of the Permian limestones occur as allochthonous blocks within the Jurassic accretionary complex of the Mino-Tanba belt in Southwest Japan. These limestone blocks are surrounded by the Middle Jurassic chaotic mudstone/sandstone matrix (e.g., Isozaki, 1997); nonetheless, within the kilometric-sized limestone blocks, the primary (pre-accretion) coherent Permian stratigraphy is retained (e.g., Sano, 1988; Ota and Isozaki, 2006).

3.1. Akasaka Limestone

The Akasaka Limestone in Ogaki city is exposed for 2 km wide in N-S and for 1 km wide in E-W (Fig. 3.2; 3.3). The Akasaka Limestone is composed of 4 stratigraphic units; i.e., the Lower, Middle, and Upper members of the Akasaka Limestone Formation plus the Ichihashi Formation, in ascending order (Akasaka Research Group, 1956; Ozawa and Nishiwaki, 1992; Zaw Win, 1999; Ota and Isozaki, 2006). All units are composed of pure bioclastic limestone with various shallow marine fossils, such as fusulines, calcareous algae, rugose corals, brachiopods, bivalves, gastropods, ostracods etc. (Zaw Win, 1999). A minor amount of dolomite is associated in the Ichihashi Fm.

The Lower Mb (over 100 m thick) consists of gray limestone, which contains fusuline of *Parafusulina granum-avenae* Roemer and *Neoschwagerina* (*Cancellina*) *nipponica* Ozawa. The base of the Lower Mb is not well exposed. The Middle Mb (ca. 70 m thick) is composed mainly of dark gray limestone and contains fusuline of *Pseudodoliolina ozawai* Yabe and Hanazawa, *Neoschwagerina craticulifera* Schwager, and *Neoschwagerina margaritae* Depart. The Upper Mb (ca. 90 m thick) consists mainly of thick-bedded black limestone. Large fusulines, such as *Neoschwagerina margaritae*, *Yabeina igoi* Morikawa and Suzuki, and *Yabeina globosa* Yabe, are common (Akasaka Research Group, 1956; Zaw Win, 1999; Kobayashi, 2011). The Ichihashi Fm (over 90 m thick) consists of light gray limestone, and abundantly yields *Codonofusiella kueichowensis* Sheng and *Reichelina changhsingensis* Sheng and Cheng (Sakagami, 1980; Ota and Isozaki, 2006). In addition, the topmost part of the Ichihashi Fm yielded Late Triassic conodonts (Matsuda, 1980); however, its

stratigraphic relationship with the underlying Permian limestone is not clear.

Fig. 3.7 shows the overall fusuline biostratigraphy of the Akasaka Limestone. On the basis of fusulines, the above-mentioned stratigraphic units are correlated as follows; the Lower Mb to the Roadian, the Middle Mb to the Roadian-Wordian, the Upper Mb to the Capitanian, and the Ichihashi Fm to the Wuchiapingian, respectively (Zaw Win, 1999; Ota and Isozaki, 2006; Kobayashi, 2011). The G-L boundary is set at the FAD horizon of the *Codonofusiella-Reichelina* assemblage, which is almost identical to the boundary between the Upper Member and the Ichihashi Fm (Ota and Isozaki, 2006). This similar assignment of G-LB in the Iwato Fm is confirmed by stable carbon isotope stratigraphy (Isozaki et al., 2007a, b).

The G-LB horizon in the Akasaka Limestone (marked by red line in Fig. 3.2) was preliminarily reported by Sakagami (1980) and Ozawa and Nishiwaki (1992), and later confirmed by Ota and Isozaki (2006). The sections described by Sakagami (1980) and Ozawa and Nishiwaki (1992) were already excavated out by mining, and the other one by Ota and Isozaki (2006) along a steep quarry surface (named NQ section in this article; Fig. 3.2) is currently out of access.

In this study, I chose two new sections in the northern part of the limestone block (KW section in the property in Kawai Lime Co. and MT section in Mitsuboshi Mining Co.; Fig. 3.2, 3.3), which were lately exposed by quarry development. In addition, I conducted scientific drilling for these 2 sections in order to obtain non-weathered fresh samples. Using rock samples both from the outcrops and drilled cores, I observed nearly 250 polished slabs and more than 450 thin sections for detailed lithofacies analysis in order to detect characteristics and patterns in appearance/disappearance of various fossils and those of the depositional setting.

3.2. Ishiyama Limestone

The Ishiyama Limestone occurs in Ono Town, Ibi County, ca. 10 km to the NNE of Akasaka (Fig 3.1). The total thickness of the Ishiyama Limestone was once estimated to be ca. 400 m; however, details are still unknown. The Ishiyama Limestone was tentatively divided into the lower, middle and upper parts, in ascending order (Fujimoto et al., 1962; Igo, 1983). The main part of the limestone is composed mostly of dark gray packstone and wackestone. In addition, the upper part accompanies light gray dolomitic limestone and also limestone conglomerate of ca. 30 m thick.

In a section along a north-facing quarry surface in the southwestern part of the limestone body (OS section; Fig. 3.5; 3.6), I described the stratigraphy of the upper and uppermost parts of the Ishiyama Limestone, and conducted scientific drilling to obtain fresh samples. I prepared nearly 150 polished slabs and 100 thin sections from this study section across the G-LB.

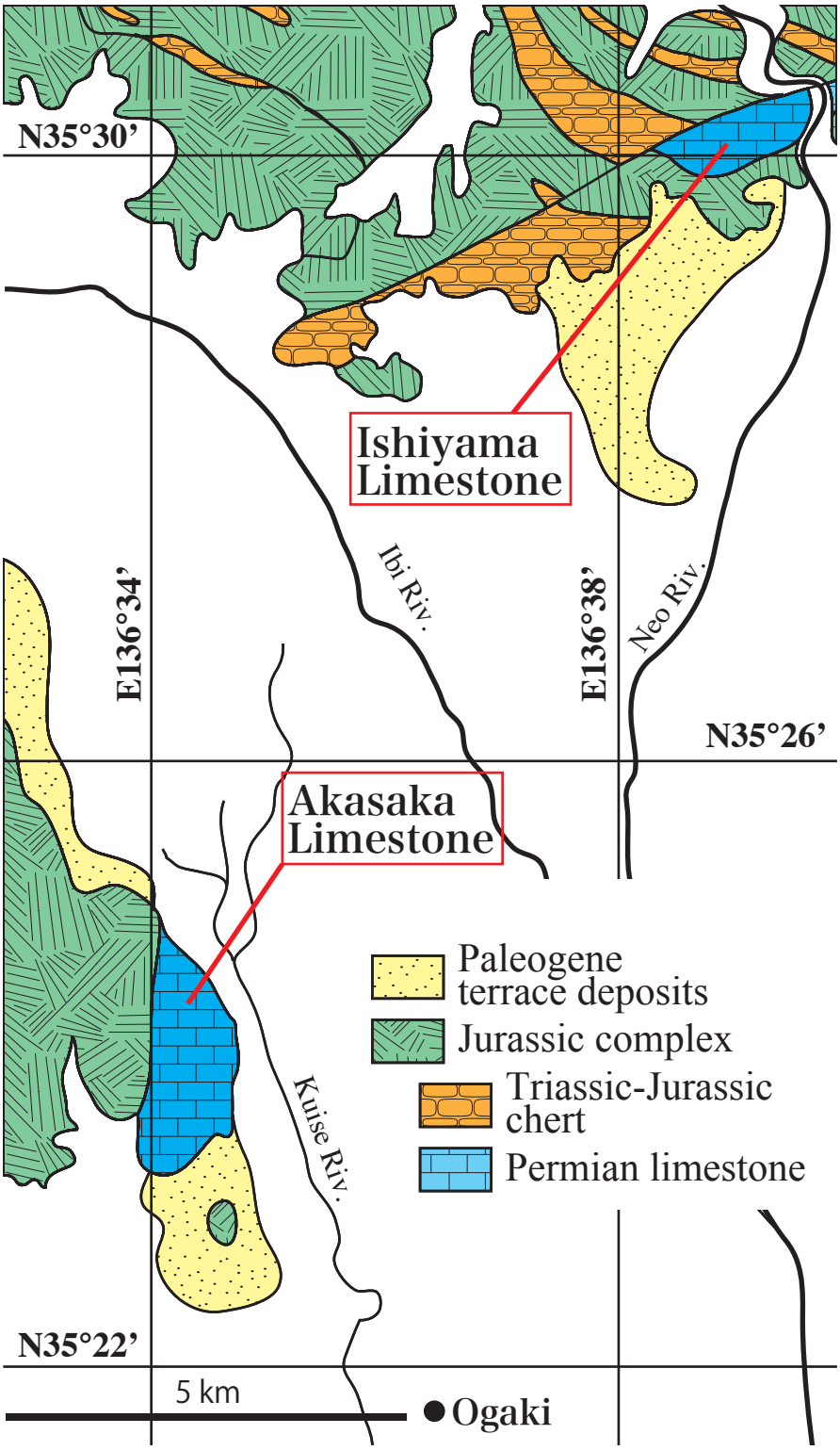

Fig. 3.1. Geologic sketch map of the Akasaka-Ishiyama area (modified from Geological Survey of Japan, AIST, 2012). Note that the Permian limestones at Akasaka and Ishiyama occur as exotic blocks within Jurassic accretionary complex.

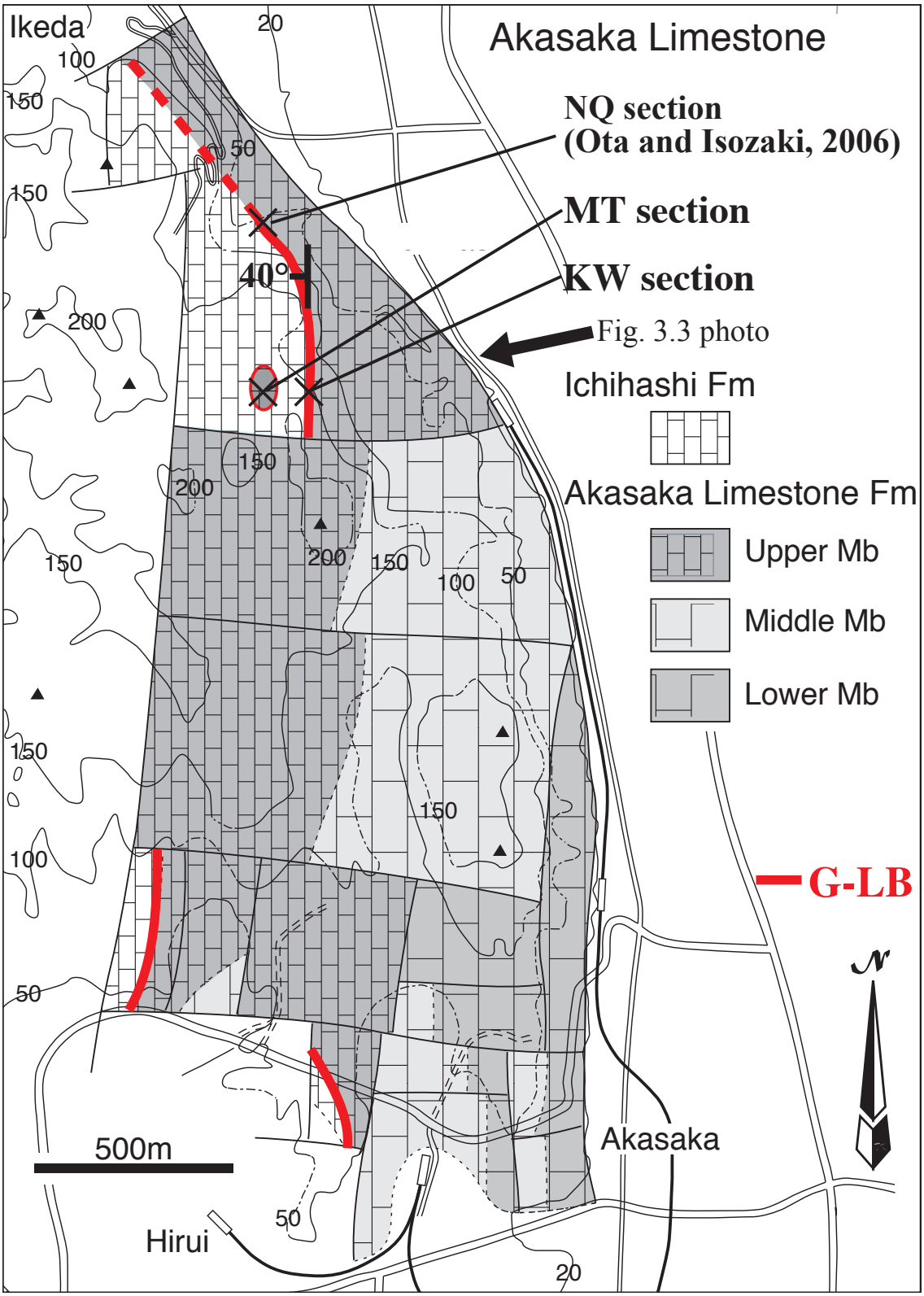

Fig. 3.2. Geologic map of the Akasaka Limestone (simplified from Akasaka Research Group, 1956) showing the locations of the studied and relevant sections. The red lines represent the G-LB horizon.

Fig. 3.3. Aerial photograph of the Akasaka limestone (by courtesy of the Mitsuboshi Mining Co.). Yellow lines show the drilled intervals at the KW and MT sections in the northern part of the limestone.

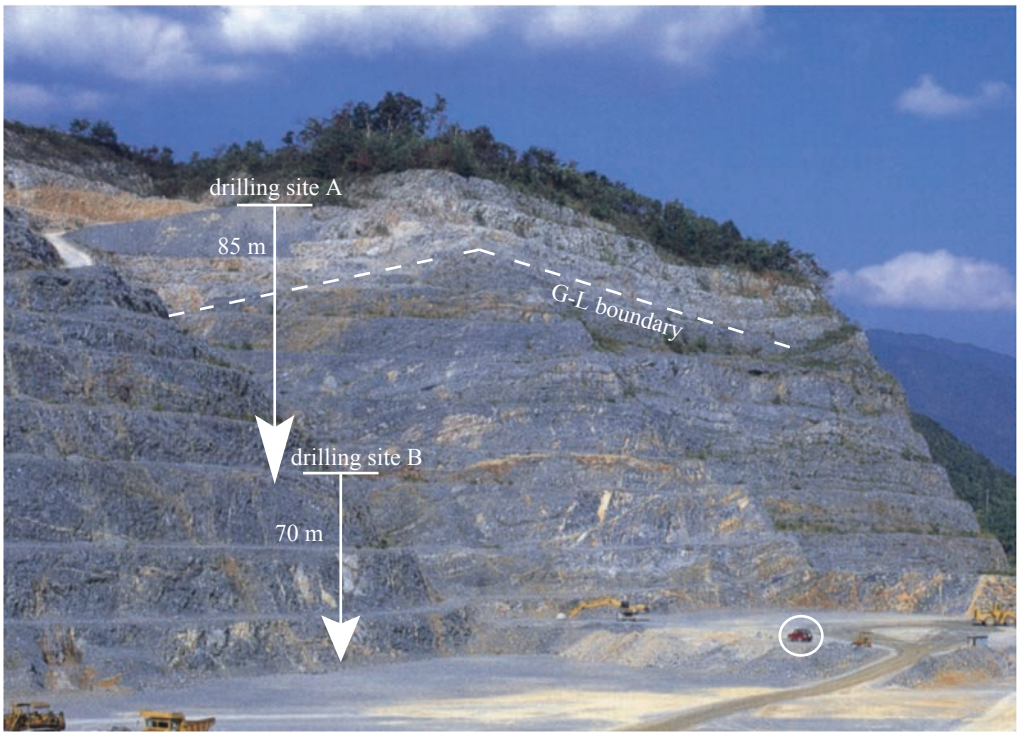

Fig. 3.4. Photograph of the KW section from the ground. Scale is a car. Black limestone (Upper Member) is overlain by light gray limestone (Ichihashi Formation). G-L boundary is located between the black limestone and the light gray limestone (dotted line). Two drilled samples were taken to attain fresh sample for chemostratigraphic study.

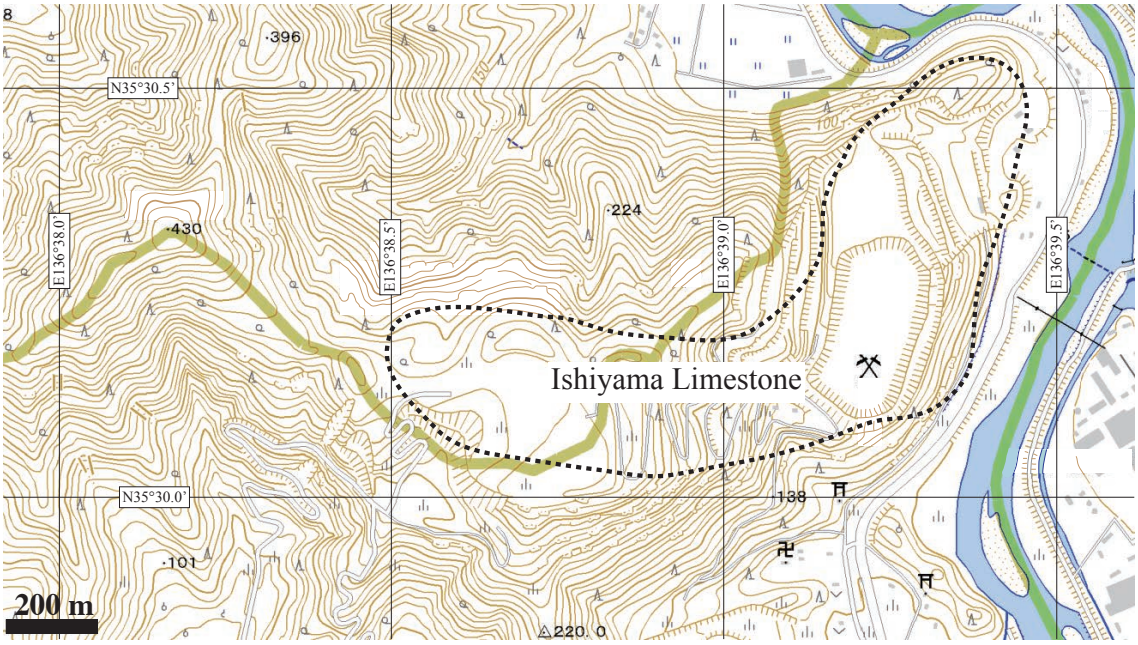

Fig. 3.5. Topographical map around the Ishiyama Limestone. The dotted line shows an Ishiyama Limestone quarry (after topographical map, Geospatial Information Authority of Japan).

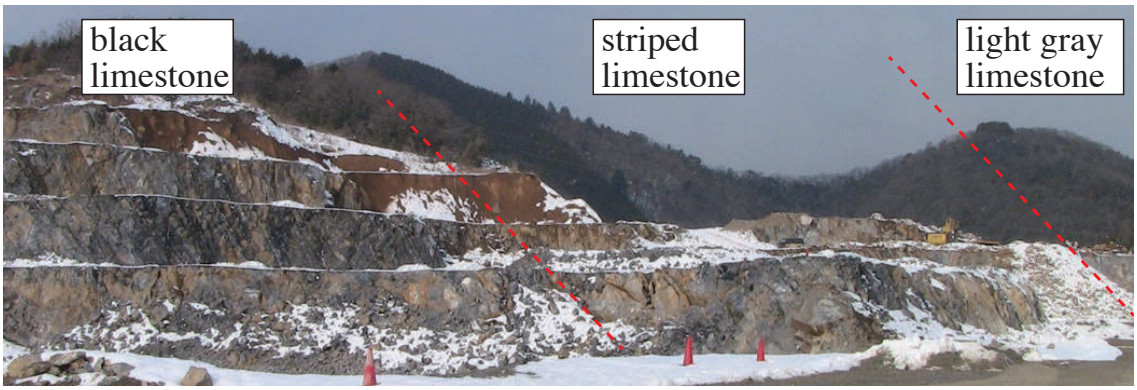

Fig. 3.6. Photograph of Ishiyama Limestone. Note that Ishiyama Limestone has almost the same litho- and biostratigraphy as those in the Akasaka Limestone.

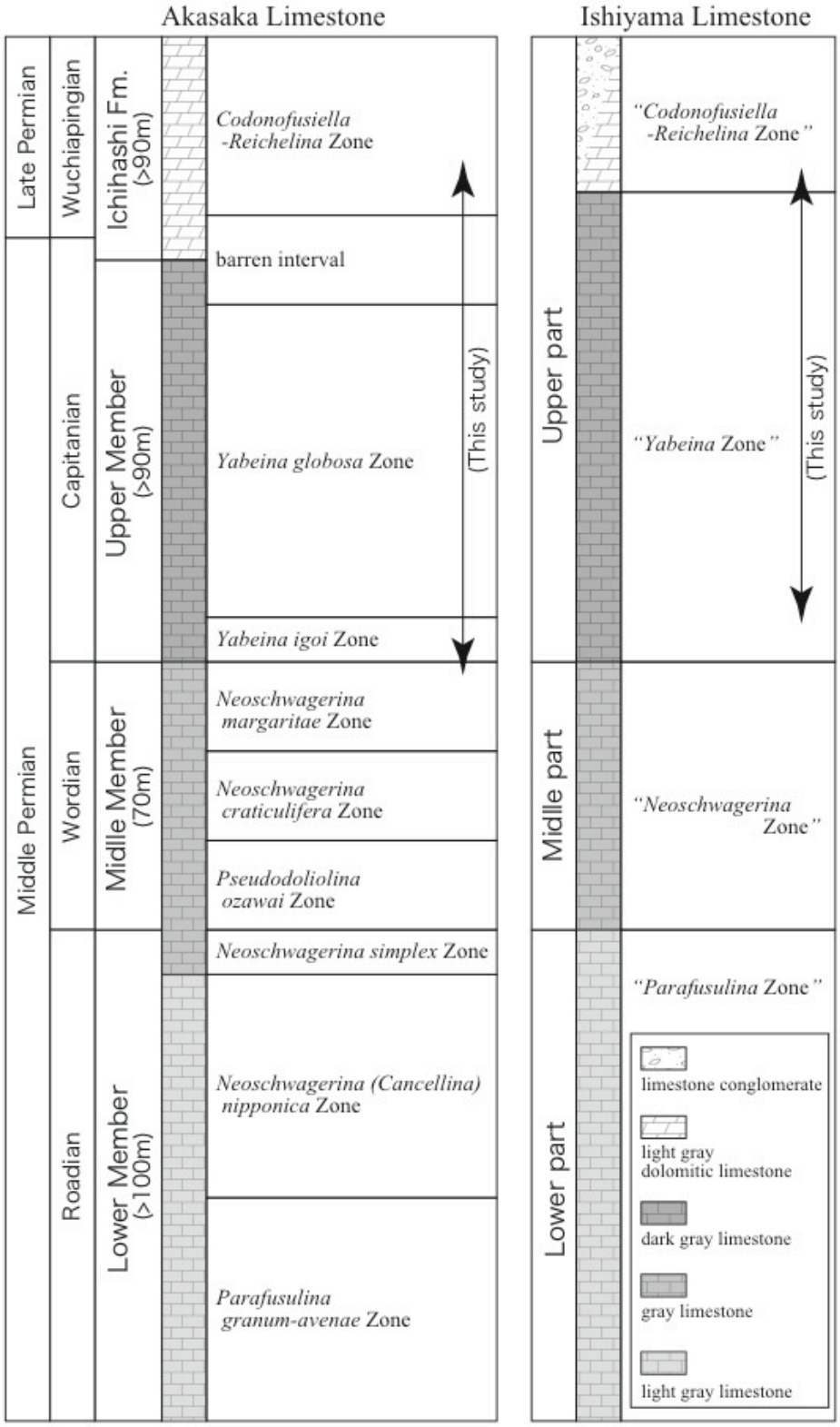

Fig. 3.7. Middle-Upper Permian fusuline zones of the Akasaka and Ishiyama limestones (after Akasaka Research Group, 1956; Fujimoto, 1962; Igo, 1983; Ozawa and Nishiwaki, 1992; Zaw, Win, 1999; Kawai, 2009; Kobayashi, 2011).

4. Litho- and biostratigraphy

4.1. Lithostratigraphy

4.1.1. KW and MT sections of Akasaka

I analyzed the G-LB intervals composed of the Upper Mb and Ichihashi Fm at 2 sections; one on an east-facing open-cut quarry surface of the Kawai Lime Co. (KW), and the other on a west-facing surface of the Mitsuboshi Mining Co (MT) (Fig. 3.3). The limestones of this interval are generally bedded (Fig. 4.1A; 4.2A; 4.3A) and consist mainly of wackestone or grainstone. They strikes in N-S and dip at 30-40° to the west (Fig. 3.2). The Upper Mb shows dark gray to black colors, whereas the Ichihashi Fm light gray (Fig. 4.3). Although multiple Miocene andesitic dykes (less than 1 m thick) penetrated into the limestone (Suzuki et al., 2011), the effect of contact metamorphism is minor in degree. Despite some small faults, the original stratigraphy of the limestone was essentially preserved.

The stratigraphic columns of the two sections are shown in Fig. 4.28. The G-LB interval consists of the following 3 units; i.e., 1) Unit B composed of black limestone (Upper Mb; over 110 m thick), 2) Unit S composed of light/dark gray striped limestone (uppermost part of the Upper Mb; 9 m thick), and 3) Unit W composed of light gray dolomitic limestone (lowermost part of the Ichihashi Fm; over 20 m thick).

4.1.1.1.Unit B: black limestone

This unit is composed of a thick pile of black limestone, and its total thickness of the black limestone at the KW section is 114 m. This unit is subdivided into 4 subunits; i.e., B1, B2, B3, and B4, in ascending order (Fig. 4.28). Each subunit consists of dark gray to black bioclastic limestone; wackestone and packstone are common with minor intercalation of grainstone. The subunits B3 and B4 are darker in color than subunits B1 and B2. Terrigenous clastics are scarcely included in the limestone.

Subunit B1 (25 m thick) mainly consists of thickly bedded (30-50 cm) dark gray limestone with flat bedding plane. This subunit consists mostly of wackestone and partly of packstone, with abundant calcareous algae (*Mizzia yabei*), large fusuline (*Neoschwagerina*, *Yabeina*), brachiopod, ostracod, smaller foraminifer, rugose coral and gastropod. In addition, large bivalve Alatoconchidae are found at two horizons. The size of the broken bivalve shells reaches 30 cm in length and 1 cm thick.

Subunit B2 (65 m thick) mainly consists of thickly bedded (30-50 cm) dark gray to black limestone with flat bedding plane. Wackestone and packstone are common with frequent intercalation of grainstone layers. Within the Unit B, the occurrence of large peloids of 50-200 μm long is unique to the grainstones. This subunit yields abundant fossils with respect to other subunits. In some layers, numerous fusulines are concentrated. Broken shells of Alatoconchidae are found at six horizons (Fig. 4.30), which are aligned parallel to bedding. Their broken shells reach up to 50 cm long and up to 2 cm thick, as photo-illustrated in Isozaki and Aljinovic (2009), indicating that individual bivalves were much larger. The bioclasts of calcareous algae were rarer than in the subunit B1.

Subunit B3 (13 m thick) mainly consists of thickly bedded (30-50 cm) dark gray to black limestone with flat bedding plane. Wackestone and packstone are common. Calcareous algae, in particular *Mizzia yabei*, occur abundantly in association with minor amounts of smaller foraminifer, brachiopod, ostracod and crinoid. Fusulines are less common and smaller in size than in subunit B2.

Subunit B4 (8 m thick) mainly consists of thickly bedded (30-50 cm) dark gray to black limestone with flat bedding plane. This subunit consists mainly of wackestone, partly of packstone or grainstone. Bioclasts of calcareous algae, smaller foraminifer, brachiopod, ostracod, crinoid, and gastropod are abundant. In contrast, large-tested fusulines are totally absent. In the uppermost 2 m-thick interval, calcareous algae, smaller foraminifer, brachiopod and gastropod occur commonly (Fig. 4.31).

4.1.1.2.Unit S: striped limestone

This unit is composed of black/white striped limestone, and its thickness is 9 m at the KW section. The contact with the underlying Unit B is conformable without any noticeable disturbance. This unit is subdivided into 5 subunits: i.e., S1, S2, S3, S4 and S5, in ascending order (Fig. 4.31). Each subunit is mainly composed of 0.5-2 cm-thick interbedded light gray and dark gray limestone, partly with cross-bedding (Fig. 4.17). The thickness of each bed varies laterally from 0.2 to 2 cm. The black part consists of grainstone or wackestone, whereas white part wackestone and partly dolomitic wackestone. Among the bioclasts, calcareous algae are most dominant with minor amounts of brachiopod, smaller foraminifer, ostracod, gastropod and crinoid. In contrast to the underlying units, fusuline, rugose coral and bivalve are absent. Smaller

foraminifer and gastropod occur only in the lowermost part (Fig. 4.31). Black part includes much more bioclasts than white part. Peloids are abundant in black part; most of them are oval to stick-like in shape and range in size of 50-200 μm in the black part.

This unit was previously described as the lowest part of the Uppermost Mb (Zaw Win, 1999) or light gray limestone of the Upper Mb (Ota and Isozaki, 2006).

Subunit S1 (4 m thick) consists of interbedded dark gray/light gray limestone beds (0.5-2 cm) with wavy bedding plane. The dark gray part consists mostly of peloidal wackestone and grainstone in part, whereas light gray part consists of sparitic wackestone (Fig. 4.9). Except the lowermost 2 m part enriched with smaller foraminifer and gastropod, calcareous algae are dominant among bioclasts, with minor amount of brachiopod, ostracod, and crinoid.

Subunit S2 (2.5 m thick) consists of massive gray, or dark gray in part, limestone, which includes discontinuous black part. Gray or dark gray part mostly consists of wackestone, but partly of sparite. Bioclasts are rare but they contain calcareous algae, crinoid, brachiopod, and ostracod in the gray or dark gray part, whereas peloids are common in the black part.

Subunit S3 (1 m thick) consists of interbedded dark gray/light gray limestone beds of 0.5-2 cm thick with wavy bedding plane. The black part consists of peloidal grainstone or wackestone, partly sparite, whereas light gray part consists of sparitic wackestone, almost the same as S1, but more sparite than S1. Fossils are very rare, but calcareous algae are common.

Subunit S4 (0.8 m thick) consists of massive gray limestone with wavy bedding plane. This limestone is composed of peloidal grainstone with few bioclasts solely of calcareous algae.

Subunit S5 (0.6 m thick) consists of interbedded dark gray/light gray limestone beds of 0.5-2 cm thick with wavy bedding plane. Dark gray part consists of peloidal wackestone or grainstone, whereas light gray part consists of sparitic wackestone. Fossils of calcareous algae, crinoid, ostracod and brachiopod are included.

4.1.1.3.Unit W: light gray dolomitic limestone

This unit is composed of light gray to white massive dolomitic limestone, and in part was heavily dolomitized, in which primary sedimentary features/fossils cannot be observed. At KW section, its thickness is over 20 m, and over 5 m at the MT section.

This unit is subdivided into 2 subunits; i.e., W1 and the overlying W2. This unit is mainly composed massive light gray to white limestone. A part of this unit is heavily dolomitized, in which fossils cannot be observed. Wackestone or grainstone are common. Subunit W1 is mainly composed of grainstone, partly wackestone. On the other hand, subunit W2 is composed of wackestone or dolomite.

Subunit W1 (6 m thick) consists of thick-bedded (20-50 cm) light gray limestone, and bedding plane is flat but wavy only at the bottom. Grainstone is common but partly wackestone is intercalated. In the grainstone, peloids are abundant. Bioclasts of calcareous algae, small fusuline, smaller foraminifer, ostracod, crinoid and brachiopod are included. At the bottom, 5 mm-thick greenish bed occurs. The detail of the bed will be described in chapter 6.

Subunit W2 (15 m thick) consists of light gray to white limestone with planer bedding. This subunit suffered heavier dolomitization than subunit W1. Wackestone and grainstone are common, and partly packstone is intercalated. This subunit yields bioclasts of calcareous algae, small fusuline, smaller foraminifer, ostracod, crinoid, rugose coral and brachiopod.

4.1.2. OS section of Ishiyama

The upper part of the Ishiyama Limestone was studied in a north-facing quarry surface in the southwestern part of the limestone block (Fig. 3.5). In addition to the conventional study of the outcrop, I conducted two drillings next to the section, as illustrated in Fig. 3.6. On the basis of the outcrop/drilled core observations, the following stratigraphy is confirmed; i.e., 1) black limestone, 2) gray limestone, 3) black/white striped limestone, and 4) light gray dolomitic limestone, in ascending order. Note that this overall stratigraphy for this ca. 55 m-thick section, and its lithologic features are quite similar to those observed at the 2 sections in Akasaka.

4.1.2.1.Black limestone

This over 37 m-thick unit consists of thick-bedded dark gray to black bioclastic limestone with planer bedding. Wackestone and packstone are common, with bioclasts of fusuline (*Neoschwagerina margaritae*, *N. minoensis*, *Yabeina katoi*, and *Gifuella* sp.), calcareous algae, large bivalve (Alatoconchidae), smaller foraminifer, brachiopod, ostracod, crinoid and gastropod. Within the topmost 0.5 m-thick interval,

large fossils are not included, except for calcareous algae and smaller foraminifers. Large bivalves (Alatoconchidae) occurred from 3 horizons, and their highest horizon is ca. 0.5 m below the top of this unit. This unit lithologically resembles thus likely corresponds to the subunits B1 to B3 of the Upper Mb of the Akasaka Limestone.

4.1.2.2.Gray limestone

This 3 m-thick unit of consists of thick-bedded gray limestone with planer bedding. The contact with the underlying black limestone is conformable without any noticeable disturbance. Wackestone and packstone are dominant with frequent intercalation of grainstone. Bioclasts include calcareous algae, smaller foraminifer, ostracod, brachiopod and crinoid. Bioclasts are more common than in the underlying upper part of the black limestone. This unit lithologically corresponds likely to the upper half of the Subunit B4 of the Akasaka Limestone.

4.1.2.3.Striped limestone

This 20 m-thick unit consists of 0.5-2 cm-thick interbedded light gray/dark gray limestone. The contact with the underlying gray limestone is conformable without any noticeable disturbance. Dark gray part contains abundant peloids and calcareous algae, whereas white part consists of lime-mud and/or sparite. The bedding is clear within the lowermost 2 m-thick part, whereas unclear within the upper part. This unit lithologically resembles thus likely corresponds to the subunits S1-S5 of the Akasaka Limestone.

4.1.2.4.Light gray limestone

This less than 6 m-thick unit consists of thick-bedded light gray dolomitic limestone. The contact with the underlying striped limestone is not clearly observed. Wackestone or grainstone are common. Bioclasts of calcareous algae, small fusuline, ostracod, and crinoid are included. This unit lithologically resembles thus likely corresponds to the subunits W1 and W2 of the lowermost Ichihashi Fm of the Akasaka Limestone.

4.1.3. Greenish bed

A unique thin bed of greenish non-carbonate nature occurs between the striped limestone of the Upper Mb and the dolomitic limestone of the Ichihashi Fm (Fig. 4.19B,

C). This peculiar bed is observed at the MT section and the NQ section previously described by Isozaki and Ota (2001); which is located ca. 500 m to the north of the MT section (Fig. 3.2). This bed forming the basal horizon of the Ichihashi Fm was previously reported as a felsic tuff by Isozaki and Ota (2001); however, details were not analyzed afterwards.

Although its thickness is less than 1 cm at the two sections, this bed is distinct from the rest of the section in various aspects. As illustrated in Fig. 4.18 and Fig. 4.19, the base of this bed is highly undulated to cut clearly the black/white banding of the topmost Subunit S5; nonetheless the bedding attitude stayed the same across this bed. This relationship recorded an erosional event immediately before the deposition of greenish bed.

This bed is composed not at all of carbonates but of extremely fine-grained clayey material less than 500 μm.

Chemical composition has not been analyzed for the greenish bed, therefore I analyzed the detailed composition of this bed by ICP-MS. In addition, there is comparable greenish bed in Kamura Limestone, southwest Japan. I also analyzed the chemical composition of this bed.

4.1.3.1.Mineralogy

The microscopic view of this bed is shown in. Figs. 4.20 and 4.21. Minerals are almost non-identifiable under the microscope. In order to identify component minerals of this greenish bed, X-ray microanalyzer and XRD analyses were made.

EPMA

Samples were analyzed by EPMA in the University of Tokyo, Komaba. Some minerals were detected and composition of minerals and matrix are analyzed. The result is shown in Table. 4.1. Matrix mainly consists of CaO (43.361-51.364 %), P_2O_5 (23.537-38.067 %), Al_2O_3 (2.110-6.293 %) and SiO_2 (2.987-10.324 %). Fine-grained minerals include three different species. One is calcite, which consists of CaO (52.716-57.529 %), probably originated from underlying limestone. Second is non-carbonate, which consists of SiO_2 (38.216-46.881 %), Al_2O_3 (13.232-31.965 %), MgO (2.706-22.990 %), CaO (0.224-7.507 %) and K_2O (0.296-9.278 %). And the third is another non-carbonate, which consists of SiO_2 (18.155 %), Al_2O_3 (6.217 %), MgO (11.504 %), CaO (28.166 %), K_2O (4.41 %) and P_2O_5 (2.274 %) (Fig. 4.22).

Especially, SiO_2 is not included in underlying limestone at all, but included only in greenish bed.

XRD chart

The greenish bed of the NQ section is analyzed by XRD in JAMSTEC, Japan. Representative XRD diagrams are shown in Fig. 4.23. The greenish bed contains only apatite, muscovite and calcite. In contrast, quartz, feldspar or plagioclase are not detected.

4.1.3.2.Chemical composition

XRF mapping

XRF mapping was done for greenish bed in Akasaka and Kamura. XRF mappings are shown in Fig. 4.24 (Akasaka) and Fig. 4.25. (Kamura). Both greenish beds are concentrated in same elements such as Si, Al, K and Cr. In contrast, underlying carbonate is concentrated in Ca and Sr.

Quantitative analysis was also done for this bed. Results are shown in Table 4.3. CaO (33.55 %), SiO_2 (33.38 %), Al_2O_3 (18.73 %) are dominant, with minor K_2O (5.09 %), MgO (2.5 %), P_2O_5 (2.02 %), Fe_2O_3 (1.79 %), TiO_2 (1.72 %) and Cr_2O_3 (1.11 %).

ICP-MS

Each sample is milled and 10 mg sample was dissolved by 200 µl $HClO_4$, HF, HCl and HNO_3. JB-3 was used for standard and reference values are after Makishima and Nakamura (2006), Makishima et al. (2002), Lu et al. (2007) and Kuritani et al. (2006).

Table 4.3 shows the result of ICP-MS analyses for greenish bed in Akasaka and Kamura (Table 4.2). Major element compositions are almost concordant with that of XRF analysis.

Rare earth element diagrams normalized by chondrite is shown in Fig .4.26 with that of Emeishan basalt and Emeishan rhyolite (Xiao et al., 2004; Xu et al., 2010). Normalized values are after Sun and McDonough (1989). Both have negative anomaly in Ce and Eu.

4.2. Biostratigraphy

Owing to the scarceness in conodont due to facies control and also due to the absence in tuff beds for radiometric dating, fusulines are the most reliable age indices for the

Akasaka and Ishiyama limestones. In this regard, there is a long list of Permian fusuline biostratigraphical studies for the Akasaka Limestone with a great variety of fusulines. Particularly as to the G-LB interval, more focused studies were attempted by Sakagami (1980), Ozawa and Nishiwaki (1992), and Isozaki and Ota (2001). Ota and Isozaki (2006) correlated the Akasaka Limestone and the Iwato Fm of the paleo-atoll origin with shelf carbonates in South China, and suggested that G-LB in the mid-oceanic limestone is assigned at the base of light gray limestone, immediately below the base of the Codonofusiella-Reichelina Zone. I add more fusuline data from the topmost Upper Mb and the lowermost Ichihashi Fm of the Akasaka Limestone, and also from the correlative interval in the Ishiyama Limestone, to confirm the previous assignment.

4.2.1. KW and MT section

From the 143 m thick KW section, fusulines occur abundantly, and I obtained specimens from 60 horizons. Among them, 4 genera and 3 species were identified. Their stratigraphic ranges are shown in Fig. 4.28. The large-tested fusuline *Yabeina globosa* is the most dominant species from the Upper Mb. This taxon occurred from the base of the core sample (B69.60) to the B3/B4 boundary horizon of the Upper Mb (Fig. 4.28) for 102 m. In Subunit B3 of the uppermost part of the black limestone, *Yabeina* occurs alone without accompanying other large-tested fusuline genera.

In contrast, no fusuline occurred from the overlying 18.7 m-thick interval; i.e. 8 m-thick Subunit B3 of the black limestone, 8.9 m-thick striped limestone (Subunits S1-S5). From Unit W above this fusuline-free interval, small-tested fusulines, such as *Codonofusiella kueichoensis* Sheng, *Reichelina chnaghsingensis* Sheng and Chang, and *Nanlingella suzukii* (Igo and Igo) occurred abundantly without large-tested ones. *Codonofusiella* sp. A reported by Ota and Isozaki (2006) is here amended to *N. suzukii* (re-identified by H. Igo). At the MT section, *N. suzukii* first appeared from Subunit W1 immediately above its base (Fig. 4.28).

On the basis of these data, the studied interval around the G-LB at KW section can be clearly divided into the following 3 zones; i.e., a zone characterized by large-tested fusulines (e.g. *Yabeina*, *Neoschwagerina*), a barren interval, a zone with small-tested fusulines (e.g., *Codonofusiella*, *Reichelina*, *Nanlingella*) (Fig. 4.28). This pattern is concordant with the previous fusuline zonation; i.e., the *Yabeina globosa* Zone, a barren

interval, and the *Codonofusiella-Reichelina* Zone (Akasaka Research Group, 1956; Sakagami, 1980; Ozawa and Nishiwaki, 1992; Zaw Win, 1999; Ota and Isozaki, 2006).

According to the previous studies (Zaw Win, 1999; Kobayashi, 2011), *Y. globosa* appeared from much lower horizon of the Upper Mb below the base of the KW section. In the KW section, therefore, the interval corresponding to the underlying *Neoschwagerina margaritae* Zone is not exposed.

According to the Permian fusuline biostratigraphic framework (e.g., Leven, 1993), the Upper Mb of the Akasaka Limestone is correlated with Capitanian, and the Ichihashi Fm with Wuchiapingian. More specifically at the KW section, Units B and S are correlated with Capitanian, and the unit W with the lowermost Wuchiapingian; therefore, the G-LB horizon in the Akasaka limestone is placed at the base of W1.

These results confirmed the previous results from the neighboring section (Ota and Isozaki, 2006). In addition, no large-tested fusulines occur in any part of the Akasaka Limestone stratigraphically above the B3/B4 boundary, therefore, the base of B4 (ca. 19 m below the G-LB) is recognized as the extinction level of all large-tested Permian fusulines.

4.2.2. OS section

Within the 68 m thick section, fusulines were recovered from 12 horizons. The stratigraphic ranges of the taxa are shown in Fig. 4.29. Among these, and 4 genera and 4 species were identified.

The OS section can be biostratigraphically divided into the following 3 intervals; i.e., one characterized by large-tested fusulines (e.g. *Neoschwagerina*, *Verbeekina*, *Yabeina*), a barren interval, and an interval characterized solely by small-tested fusulines (*Nanlingella*). According to Fujimoto et al. (1962), the lower part (> 80 m thick) consists of light gray to white limestone and yields *Parafusulina* and *Pseudodoliolina* abundantly. The middle part (70 m) consists of dark gray to light gray limestone and yields *Neoschwagerina*. The black limestone of the upper part (>260 m) yields *Yabeina*, whereas the light gray dolomitic limestone and limestone conglomerate yield *Codonofusiella* and *Reichelina*. Our result is concordant with the previous reports (Fujimoto, 1962; Igo, 1983; Kawai, 2009).

These fusulines indicate that the Ishiyama Limestone ranges in age from the Roadian to Wuchiapingian. The dark gray limestone of the upper part is correlated with

Capitanian, and the dolomitic limestone with Wuchiapingian, respectively. Although the occurrence of index fusulines are relatively rare, the G-LB horizon likely occurs at the boundary between the striped limestone and the dolomitic limestone of the upper part of this limestone body as in the cases of the KW and MT sections in the Akasaka Limestone described above.

4.3. Change in fossil abundance across the G-LB

In general, the Lower to Upper members of the Akasaka Limestone demonstrates the highest faunal diversity as previously reported in many studies (e.g., Zaw Win, 1999). In contrast, the overlying transitional interval and the Ichihashi Fm show clearly less divergent faunal composition (Ota and Isozaki, 2006). This dramatic change includes the major extinction of representative shallow marine biota, such as large-tested fusulines, rugose corals, and large bivalves immediately before the G-LB. This pattern is more or less the same in the Ishiyama Limestone.

On the basis of the observation of 450 thin sections, I analyzed stratigraphic change in abundance of fossils in the upper part of the Upper Mb and the transitional interval across the G-LB of the KW section. Within the black limestone (Subunits B1-B4), calcareous algae, mollusks (bivalves, gastropods), brachiopods, ostracods, corals, crinoids, and foraminifers occur commonly, as shown in Figs. 4.30 and 4.31.

Calcareous algae (*Mizzia yabei*) remained dominant throughout the section. Large fusulines, smaller foraminifers, and bivalves are abundant particularly in Subunit B2 (Fig. 4.30). On the other hand, above the Subunit B3/B4 boundary, large fusuline and large bivalve disappear completely. The last occurrence of rugose coral in the KW section is in the middle of Subunit B2. They never returned in the overlying strata, clearly indicating that a significant change in faunal composition occurred during the deposition of the upper part of black limestone, particularly somewhere around the B3/B4 boundary, as illustrated in Fig. 4.30.

In addition, another change in faunal composition was recognized in the lower part of the striped limestone (Subunit S1) (Fig. 4.30). At this horizon, all gastropods and smaller foraminifers disappeared, and ostracod significantly declined (Fig. 4.30). Small-tested fusulines, smaller foraminifers, and molluscs are totally absent except for the lower part of Subunit S1.

The present study focusing on the G-LB event clarified that the disappearance of

major Capitanian taxa occurred virtually in two steps; i.e., the first disappearance of large-tested fusulines at Subunit B3/B4 boundary, and the second episode of smaller foraminifer and molluscs in the basal part of Subunit S1. Accordingly the previously assigned "barren interval" by Ota and Isozaki (2006) can be divided into two subintervals; the lower half of the barren interval from the base of Subunit B4 to the lower part of Subunit S1 (ca. 11 m thick) and the upper half from the lower Subunit S1 to the base of Subunit W1 (ca. 9.5 m thick). Thus the significant biodiversity drop during the latest Capitanian in fact involved the two-stepped change in faunal composition.

Accordingly, the upper part of Subunit S1 and Subunit S2 represent an interval characterized by the lowest biodiversity of shallow marine animals in the KW section. Nonetheless, it is noteworthy that calcareous algae became relatively dominant in the striped limestone with respect to the black limestone of Subunit B4.

On the other hand, the first appearance of Late Permian fusuline and smaller foraminifer was recorded in the Subunit W1 in the lower part of light gray limestone, which marks the base of the *Codonofusiella-Reichelina* Zone, thus the biostratigraphically defined G-LB (Figs. 4.28, 4.30). This horizon is placed about 20 m above the B3/B4 boundary, and even 9.5 m above the second diversity drop; therefore, the biodiversity drop of the Capitanian fauna occurred clearly before the G-LB.

Above the lowest diversity interval, the first appearance of the Wuchiapingian assemblage was marked at the basal part of the dolomitic limestone of Subunit W2. Nonetheless, the diversity was still not in full recovery aspect solely with small-sized foraminifers, as demonstrated in Fig. 4.30.

The overall transition patterns of fossil abundance in the G-LB interval at the MT section in Akasaka and the OS section in Ishiyama are more or less the same as that of the KW section.

4.4. Discussion

The composition with pure carbonates including many bioclasts of shallow-marine organism, in particular with those characterizing photosynthesis and/or photosymbiosis, and the terrigenous clastics-free nature undoubtedly guarantee the origin in paleo-atoll complex developed on the top of a paleo-seamount.

4.4.1. Irreversible change in depositional setting in shallow mid-superocean around the G-LB

The composition with pure carbonates including many bioclasts of shallow-marine organism, in particular with those characterizing photosynthesis and/or photosymbiosis, and the terrigenous clastics-free nature undoubtedly guarantee the origin in paleo-atoll complex developed on the top of a paleo-seamount.

4.4.1.1.Subtidal setting of Unit B

The ubiquitous occurrence of calcareous algae (*Mizzia*) and associated photosymbiotic large-tested fusulines (*Yabeina*) throughout Unit B (Fig. 4.30) clearly recorded that the depositional site was in extremely shallow water in the euphotic zone. Nonetheless, the dominance of wackestone and packstone, i.e., that of lime mud matrix (Fig. 4.5), indicates that the Unit B was essentially deposited in a quiet sedimentary setting. Although the unworn nature of fusuline bioclasts with minor abraded ones, and the periodical intercalation of grainstone imply the occasional input of coarse-grained bioclasts probably by high-energy flow, all these lines of evidence indicate that the black limestone of Unit B was probably deposited in the subtidal zone. In the mid-oceanic setting, the central lagoon of an atoll complex is the only possible candidate for such low-energy shallow environments. This interpretation is essentially the same as that by Zaw Win (2000) for the Capitanian part of the Akasaka limestone.

The change from Subunit B3 to B4 is not conspicuous because Subunit B3 and the lower part of Subunit B4 have quite similar lithofacies except for the difference in composition of bioclasts. The boundary, however, marks the clear extinction horizon of large-tested fusulines (Fig. 4.31). This suggests that the biodiversity decline occurred regardless of major change in lithofacies. Above this level, in contrast, the amount of lime-mud matrix decreases upsection into the upper part of Subunit B4, implying the shift into a relatively higher-energy environment. The depositional setting likely became gradually shallower during the deposition of Subunit B4. The overall change from the black limestone (Subunit B4) to the overlying striped limestone (Subunit S1) is also gradual.

4.4.1.2.Intertidal setting of Unit S

The development of remarkable large-scale cross-bedding (Fig. 4.17) is restricted to the Unit S. This indicates an extremely shallow high-energy environment characterized by the constant water agitation. In addition, the erosional surface occurred at the top of the Unit S (Figs. 4.18, 4.19), indicating that this likely reflected the further shallowing of depositional setting upsection. Nonetheless, no evidence was observed for the supratidal environment, such as evaporite and birds-eyes structure. Most of Unit S was deposited probably in the intertidal zone.

Subunits S1, S3, and S5 consist of the unique striped sparitic limestone with remarkable cross-bedding (Fig. 4.17), whereas Subunits S2 and S4 are composed of wackestone with less clear striped pattern and lacks cross-bedding. The contrast between these two groups likely reflected the difference in water-depth; i.e., the former likely represents relatively shallower condition than the latter. I interpret that Subunits S1, S3, and S5 represents the upper intertidal zone, whereas Subunits S2 and S4 the lower intertidal zone, respectively. During the deposition of Unit S, minor fluctuations in sea-level likely occurred for multiple times in the extremely shallow part of the Akasaka paleo-atoll complex. Zaw Win (2000) previously mentioned that the correlative interval to Unit S was deposited in the shallower intertidal zone with eventual exposure to supratidal conditions.

4.4.1.3.Inter-subtidal setting of Unit W

The dominance of grainstone and absence of lime-mud matrix in W1 (Fig. 4.15) indicate high-energy depositional setting. In contrast, W2 is composed mostly of sparitic wackestone or packstone and partly grainstone (Fig. 4.16). However, most part suffered heavy dolomitization, resulting in loss of original texture. Therefore, the depositional setting of W2 is unclear, but probably slightly deeper than W1. In addition, cross-bedding like Unit S does not occur. Therefore, the depositional setting of W1 might have been the intertidal zone, whereas that of W2 subtidal zone. This pattern is concordant with the subaerial exposure at the Unit S/Unit W transition. Zaw Win (2000) interpreted that the Wuchiapingian dolomitic limestone in Akasaka might have been exposed in the supratidal zone, but no evidence indicating supratidal environment was shown.

4.4.1.4.Erosion around the G-LB

The lithological difference is remarkable between Unit S and Unit W, not only in color but also in components/textures (Fig. 4.14). In this regard, it is noteworthy that the top of Subunit S5 was sharply cut by an erosional surface as observed at the MT section (Fig. 4.18). This clearly recorded the subaerial exposure and erosion of the topmost Unit S. Across the boundary between these two units, an abrupt facies change likely occurred in the extremely shallow-water setting on the top of the paleo-atoll complex of Akasaka.

4.4.1.5.Overall trend

By summarizing above discussion on the KW section, the history of the Capitanian to Wuchiapingian relative sea-level change detected in the Akasaka limestone is reconstructed as follows; i.e., 1) during most of the Capitanian, shallow marine limestone was deposited continuously in the subtidal setting, 2) the depositional site shifted into the intertidal zone in the latest Capitanian, then 3) subaerially exposed/eroded immediately before the G-LB, and consequently 4) returned to the intertidal setting across the G-LB and afterwards in the Wuchiapingian (Fig. 4.35). The MT section recorded nearly identical stratigraphy and lithofacies with Unit S and Unit W of the KW section. The OS section at Ishiyama also shares almost the same stratigraphy and lithofacies as those of Akasaka limestone (Fig. 4.29). The above-summarized sequence of changes, therefore, represents the general trend of the Capitanian-Wuchiapingian mid-Panthalassan paleo-atoll carbonates.

The three analyzed Permian limestones around the G-LB horizon, i.e. KW and MT sections in Akasaka and the OS section in Ishiyama, are litho- and bio-stratigraphically correlated with each other as described above. Their common stratigraphy positively suggests that the Permian shallow marine carbonates of these 3 sections were deposited in almost identical setting around the G-LB timing.

Among all, the latest Capitanian erosion-related hiatus is the most significant feature because this marks the relatively lowest sea-level in the entire Capitanian-Wuchiapingian interval in the mid-Panthalassan record.

4.4.2. Biotic Response to environmental stress

The present analysis, particularly that for the KW section, documented the distinct stratigraphic change in fossil composition in two steps during the latest Capitanian (Figs. 4.30, 4.31). This likely suggests that the ambient environments on the top of mid-oceanic seamount have changed in two steps. In this section, the response of shallow-marine biota to the two-stepped environmental change is discussed with respect to possible cause(s).

4.4.2.1.First episode: end of gigantism

First at the Subunit B3/B4 boundary in the upper Capitanian, large-tested fusuline genera, such as *Yabeina*, *Neoschwagerina*, *Chusenella*, and *Gifuelloides* as well as large bivalves (Alatoconchidae) totally disappeared (Fig. 4.30). The diversity decline of large-tested Middle Permian fusulines in fact started during the Wordian to early Capitanian (e.g., Zaw Win, 1999; Kobayashi, 2011), much earlier than the G-LB. Nonetheless, it is significant that all of the Permian long-ranging, large-tested fusulines (Schwagerinidae, Verbeekinidae) totally became extinct at this level and never returned afterwards. This sharp disappearance of large-tested fusulines together with large bivalves suggests that a significant, in particular, highly stressful environmental change has likely appeared in the late Capitanian in the low-latitude mid-Panthalassa.

The Permian large-tested fusulines and extraordinarily large bivalves are generally regarded to have lived in photosymbiosis with algae (e.g., Ross, 1967; Seilacher, 1990; Isozaki, 2006; Isozaki and Aljinovic, 2009). These Permian photosymbiosis-dependent fauna were likely adapted to extremely warm, shallow-marine settings probably of oligotrophic conditions in the low-latitude, tropical zone. The atoll settings on the top of paleo-seamounts provided such a hospitable conditions for shallow-marine biota throughout most of the Permian until the latest Capitanian when an acute change occurred to terminate their favorable settings. The disappearance of rugose corals (another long-ranged Permian lineage) in the Subunit B3, and the sharp diversity loss of calcareous algae at the Subunit B3/B4 boundary of the KW section (Fig. 4.30), also indicate the suppression/re-organization of photosymbiosis-dependent biota. As in the modern tropical shallow-marine environments, photosymbiosis-dependent gigantism is an adaptation to oligotrophic

conditions. The appearance of a eutrophic condition might be a candidate that terminated the Capitanian gigantic biota (Isozaki and Aljinovic, 2009).

4.4.2.2.Second episode: the onset of severest stress

The present study documented another remarkable horizon of biotic elimination within the lower Subunit S1; i.e., the disappearance of smaller foraminifers and gastropods (Fig. 4.31). Both lineages re-appeared after the G-LB; however, most of Subunit S represents a distinct interval without eye-catching fusulines and bivalves, i.e., an exceptional mollusk- and foraminifer-free interval within the highly fossiliferous Akasaka limestone. This upper half of the barren interval is thus regarded to have represented the duration of the most stressful conditions in the history of the Akasaka paleo-atoll biota.

In contrast, immediately above the G-LB hiatus, fusulines re-appeared abundantly (Figs. 4.20, 4.30). Nonetheless, all of the individuals are significantly small in size, as previously pointed out by Ota and Isozaki (2006). Although these fusulines are not the same as the gigantic ones of the Capitanian, this phenomenon apparently looks like the post-extinction "Lilliput syndrome" sensu lato (Isozaki and Aljinovic, 2009). Under a stressful condition, large individuals are often times eliminated preferentially, whereas survivors are limited to small-sized individuals.

4.4.2.3.Algal response

The Permian calcareous algae behaved differently from other contemporary protists and animals in the Akasaka paleo-atoll complex. As shown in Figs. 4.30, 4.31, the Akasaka limestone constantly yields calcareous algae from almost all horizons, indicating that algal photosynthesis worked properly regardless of the turmoil of protists and animals in the same shallow-marine environments on the top of paleo-seamount. Calcareous algae indeed became less abundant in the barren interval", i.e., Subunits B4 and S1-S3, although any distinct extinction event was not detected (Fig. 4.31).

It is noteworthy, however, that this stratigraphic change in floral assemblage in the Akasaka limestone occurred not in harmony with that of protists and animals. The representative algal genus from the Akasaka limestone is *Mizzia* (Dasycladacean green algae) in association with less abundant *Permocalculus*, *Gymnocodium*, *Eogoniolina* (green algae) etc. (Endo, 1953, 1954). In particular, within Unit B except for Subunit

B4, *Mizzia* was consistently dominant, whereas *Mizzia* totally disappeared during the deposition of Subunit B4, and in turn, *Permocalculus* took over. This change occurred independently on the sedimentary facies change, because Subunit B3 and B4 were deposited in similar subtidal settings. *Mizzia* immediately returned at the base of Unit S, and kept its continuous occurrence upsection into Unit W without showing any significant change across the G-LB hiatus. The short-term suppression of *Mizzia* growth limitedly during the deposition of Subunit B4 is one of the most interesting aspects of the Akasaka biota for discussing the latest Capitanian environmental change; however, further analysis is needed for explaining such a unique algal response in the terms of limiting factors of marine algal growth; e.g. temperature, nutrients, salinity etc.

4.4.3. Late Capitanian sea-level drop

The putative environmental stress that appeared in the late Capitanian has not yet been identified; nonetheless, the sedimentary characteristics discussed above provide some clues. The overall trend of facies change (Fig. 4.34) suggests a relative sea-level drop in the latest Capitanian to the earliest Wuchiapingian across the G-LB. The long-term dominant and stable subtidal facies of Unit B was terminated abruptly at the B/S unit boundary, and intertidal facies took over in the Unit S of the uppermost Capitanian into the Unit W of the lowermost Wuchiapingian. Furthermore, the detection of a clear erosional surface at the Unit S/W boundary (Figs. 4.18, 4.19) proves that a significant sea-level drop has occurred at the top of the Akasaka paleo-seamount to mark an intermission of atoll carbonate deposition. This agrees with the overall shallowing trend in facies of the upper Capitanian. Although the magnitude of sea-level drop is difficult to estimate precisely, the facies change from a subtidal at least to a supratidal (above-sea-level) setting requires a drop of more than several meters.

It is noteworthy that such a remarkable sea-level drop was never detected in the rest of the Akasaka limestone, thus it marks a major change in the continuous depositional record of the Akasaka paleo-atoll complex in mid-Panthalassa. The lithostratigraphy and facies change of the Ishiyama limestone (Fig. 4.29) appear identical to those of the Akasaka limestone as to the same interval. In addition, those of another Permian paleo-atoll complex at Kamura in central Kyushu recorded the same trend and attitudes, regardless of its current physiological separation of ca. 500 km to the west from Akasaka (Fig. 1.7). As the paleo-atoll complex in Kyushu was derived obviously from

an independent but from a neighboring on in the same seamount chain, the low-latitude domains of mid-Panthalassa have ubiquitously experienced a significant sea-level drop at the end of Middle Permian.

In general, mid-oceanic seamounts start sinking immediately after their birth at hotspots according to the Sclater's Law for an oceanic plate, whereas on the top, shallow-marine reefy carbonates keep growing upward to fulfill the overlying accommodation space. A remarkable lowering of sea-level of a global context is inevitable, rather than the uplift of seamount itself, to explain remarkable atoll-erosion, such as the one I detected in the Permian Akasaka paleo-atoll complex.

Although no such phenomenon has been previously reported from the lost Permian superocean, a large-scale sea-level drop at the end of Capitanian has been globally recognized through conventional sequence stratigraphic analyses of continental shelf deposits accumulated around Pangea (Fig. 1.5). Many Permian sections in South China have a remarkable unconformable between Capitanian and Wuchiapingian; e.g., the Chaotian section in northern Sichuan with plural missing conodont zones below the G-LB (Isozaki et al., 2008; Saitoh et al., 2013). This was the main reason why the Penglaitan section in Guanxi with rarely preserved continuous strata was chosen for the GSSP (global stratotype section and point) of the G-LB (Jin et al., 2006).

Furthermore, the trend agrees with the Permian global eustatic curve reconstructed on the basis of sequence stratigraphic data (Haq and Shutter, 2008), in particular, with the first order cycle punctuated by the lowest sea-level immediately before the G-LB (Fig. 6.1). Indeed, the lowest sea-level of the Phanerozoic, even lower than the Quaternary average, was recorded at the end of the Capitanian. In South China, the regional hiatus across the G-LB was blamed to the regional uplift owing to the Emeishan plume emplacement (He et al., 2003); nonetheless, the global lowering of sea-level cannot be ignored as the background cause of the hiatus also in South China.

After all, the sea-level drop detected around the G-LB in the Akasaka Limestone (Fig. 4.35) likely reflected this global signature. The present results from the Akasaka paleo-atoll from mid-Panthalassa not only demonstrate for the first time that the sea-level drop occurred in the mid-oceanic realm but also that the late Capitanian sea-level drop was indeed of global context.

4.4.4. Origin of the greenish bed

The occurrence of typical non-carbonate silicate bed around the G-LB in the Akasaka and Kamura limestones is very important, because non-carbonate is rarely deposited on mid-oceanic atoll complex. Furthermore, non-carbonate bed occurs only one horizon in Permian around Akasaka and Kamura area. Therefore, unusual source for this bed is expected around the G-LB.

In south China, which was the nearest continent from the Akasaka seamount in the Permian, "Wangpo tuff" is prevalent around the G-LB horizon (e.g. Lu et al., 1956; Saitoh et al., 2013).

Another possible source is Emeishan flood basalt. Emeishan flood basalt erupted in the earliest Wuchiapingian clearly above Wangpo tuff.

Greenish bed in the Akasaka Limestone does not include zircon or quartz which generally occur in the felsic volcanism. However, indirect evidence is a ternary plot of La-Th-Sc, indicating felsic source rather than mafic source (Fig. 4.36). In addition, mafic volcanism is generally moderate, thus volcanic ash cannot reach the mid-oceanic seamount (Isozaki et al., 2007). Further inspections are needed for the greenish bed, but until now, felsic volcanism was likely the source of the greenish bed.

Table. 4.1. Major element analysis for greenish bed in MT section by EPMA.

	SiO_2	TiO_2	Al_2O_3	Cr_2O_3	FeO	MnO	NiO	MgO	CaO	Na_2O	K_2O	P_2O_5	Total
matrix													
1	2.987	0.137	2.110	0.043	0.067	0	0.015	0.212	51.364	0.037	0.724	38.067	95.760
2	6.587	0.056	3.897	0.096	0.038	0.006	0.013	0.446	48.076	0.069	1.295	35.557	96.136
3	5.314	0.010	3.416	0.106	0.029	0	0.001	0.410	49.595	0.063	0.986	36.684	96.664
4	4.523	0.046	2.652	0	0	0	0.024	0.328	50.258	0.063	0.986	37.628	96.508
5	5.272	0.029	2.889	0.153	0.032	0.032	0	0.411	46.161	0.068	1.221	23.537	79.805
6	4.613	0.020	2.893	0.053	0.043	0.032	0.025	0.324	49.562	0.063	0.921	37.152	95.701
7	10.234	0.541	6.293	0.139	0.197	0	0.041	0.557	43.361	0.085	2.129	32.599	96.176
Avg.	5.647	0.120	3.450	0.084	0.058	0.010	0.017	0.384	48.340	0.064	1.187	34.461	
calcite													
1	0	0	0	0.022	0.028	0.121	0	0.246	55.445	0	0	0.391	56.253
2	0	0	0	0.113	0.033	0	0.016	0.688	57.000	0.028	0.011	0.553	58.442
3	0	0	0.069	0.039	0.026	0	0	0.146	55.685	0	0.047	0.430	56.442
4	0	0	0.043	0	0.008	0.002	0.001	0.128	57.529	0.008	0.068	0.470	58.257
5	0	0	0	0.042	0.052	0.136	0	0.238	55.696	0.015	0.051	0.543	56.773
6	0.571	0	0.344	0	0.217	0.054	0	2.231	52.716	0	0.300	0.414	56.847
Avg.	0.095	0	0.076	0.036	0.061	0.052	0.003	0.613	55.679	0.009	0.080	0.467	
non-carbonate mineral 1													
1	38.216	0.030	21.022	0.568	0.907	0.013	0.028	22.753	0.332	0.015	1.528	0.106	85.508
2	41.452	0.118	13.494	0.468	2.423	0.049	0	21.500	0.449	0.070	8.392	0.160	88.575
3	44.400	0.042	24.808	0.582	0.091	0	0.004	2.937	7.057	0.075	8.079	6.367	94.442
4	44.961	0.042	25.816	0.714	0.176	0.001	0	2.706	5.414	0.061	8.438	4.688	93.017
5	42.224	0.120	14.105	0.621	1.353	0.028	0.013	21.856	0.405	0.043	7.451	0.087	88.306
6	42.219	0.065	24.801	0.247	0.330	0	0.006	13.368	1.011	0.030	0.562	0.597	83.236
7	46.881	0.093	31.965	0.174	0.464	0	0	3.531	0.618	0.074	1.164	0.160	85.124
8	42.233	0.165	13.232	0.529	1.143	0	0.003	22.523	0.391	0.071	8.958	0.131	89.379
9	43.061	0.021	23.599	0.156	0.663	0	0.043	11.152	0.464	0.027	4.378	0.141	83.705

Table. 4.1. (Continued)

	SiO_2	TiO_2	Al_2O_3	Cr_2O_3	FeO	MnO	NiO	MgO	CaO	Na_2O	K_2O	P_2O_5	Total
10	41.378	0.057	14.044	0.496	1.339	0	0.015	22.990	0.224	0.059	9.278	0.071	89.951
11	40.339	0.182	14.706	0.955	2.715	0.015	0	20.891	0.329	0.085	9.249	0.113	89.579
12	39.930	0.037	26.781	0.366	1.633	0.019	0	14.383	0.530	0.004	0.296	0.137	84.116
13	42.866	0.059	13.487	0.307	1.468	0.011	0	21.151	0.239	0.039	8.209	0.107	87.943
Avg.	42.320	0.079	20.143	0.476	1.131	0.010	0.009	15.519	1.343	0.050	5.845	0.990	
non-carbonate mineral 2													
1	18.155	0.560	6.217	0.180	0.661	0.039	0	11.504	28.166	0	4.41	2.274	72.166

Table. 4.2. Quantitative analysis for greenish bed in the NQ section of the Akasaka Limestone.

	wt %		wt %
Mg	1.31	MgO	2.5
Al	9.91	Al_2O_3	18.73
Si	15.6	SiO_2	33.38
P	0.88	P_2O_5	2.02
K	4.23	K_2O	5.09
Ca	23.98	CaO	33.55
Ti	1.03	TiO_2	1.72
Cr	0.76	Cr_2O_3	1.11
Fe	1.25	Fe_2O_3	1.79
Rb	0.04	Rb_2O	0.05
Sr	0.02	SrO	0.02
Zr	0.02	ZrO_2	0.03
O	40.76		

Table 4.3. Akasaka Limestone and Kamura Limestone. a) Makishima and Nakamura, 2006, b) Makishima et al., 2002, c) Lu et al., 2007, d) Kuritani et al., 2006.

	Akasaka		Kamura		Reference
	wt %	stdev(%)	wt %	stdev(%)	
Na_2O	0.09	4.19	0.09	3.64	a)
MgO	0.92	3.39	1.10	2.96	a)
Al_2O_3	8.07	3.51	9.32	3.83	a)
K_2O	2.32	3.87	0.27	3.43	a)
CaO	39.92	3.77	50.84	3.52	a)
TiO_2	1.16	1.33	0.42	1.25	c)
MnO	0.01	2.49	0.01	2.16	a)
Fe_2O_3	0.95	2.68	0.97	2.46	a)
	ppm	stdev(%)	ppm	stdev(%)	
Sc	10.26	4.56	5.54	5.20	a)
V	130.68	3.59	286.62	3.24	a)
Cr	1847.09	3.21	1748.78	3.03	b)
Co	2.30	11.18	3.80	9.69	a)
Ni	21.09	6.64	28.17	7.26	b)
Cu	46.86	3.41	12.10	5.00	b)
Zn	74.73	3.49	44.58	4.10	b)
Ga	10.40	3.19	8.00	3.73	a)
Rb	98.29	2.78	21.61	2.67	a)
Sr	416.42	2.75	610.32	2.54	a)
Y	107.73	2.80	62.49	2.73	a)
Zr	220.99	2.80	46.84	2.98	c)
Nb	29.90	2.28	12.74	1.88	c)
Cs	5.34	2.10	12.17	1.80	a)
Ba	189.39	3.09	127.73	2.91	a)
La	111.20	2.14	228.97	1.77	a)
Ce	67.52	2.16	102.40	1.77	a)
Pr	23.89	2.14	29.83	1.80	a)

Table 4.3. (Continued)

	Akasaka		Kamura		Reference
	ppm	stdev(%)	ppm	stdev(%)	
Nd	102.63	2.14	114.62	1.84	a)
Sm	16.17	2.22	14.95	1.92	a)
Eu	2.73	2.26	2.16	1.96	a)
Gd	13.32	2.42	13.65	2.23	a)
Tb	1.63	2.26	1.49	2.19	a)
Dy	9.52	2.19	7.83	1.92	a)
Ho	2.03	2.13	1.48	1.98	a)
Er	5.88	2.18	3.70	2.05	a)
Tm	0.82	2.21	0.45	2.09	a)
Yb	5.61	2.28	2.63	2.17	a)
Lu	0.97	2.23	0.39	2.20	a)
Hf	3.88	2.15	1.34	2.12	c)
Ta	1.50	2.14	0.67	1.93	c)
Pb	25.47	1.98	5.39	1.57	d)
Th	35.92	2.25	11.64	1.63	d)
U	10.36	2.22	16.39	1.74	d)

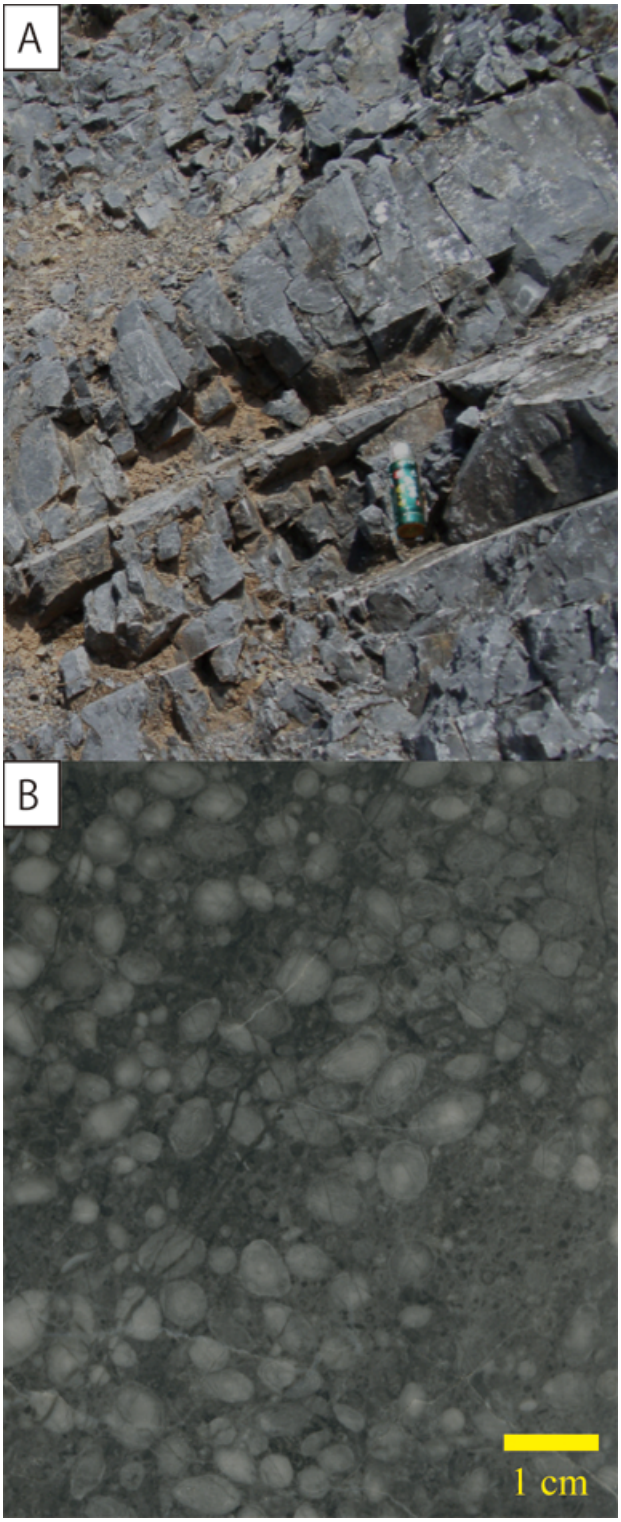

Fig. 4.1. Photograph of outcrop (A) and polished slab (B) of the black limestone. Note that this part is thickly bedded, and includes large fusulines (e.g. *Yabeina*, *Neoschwagerina*)

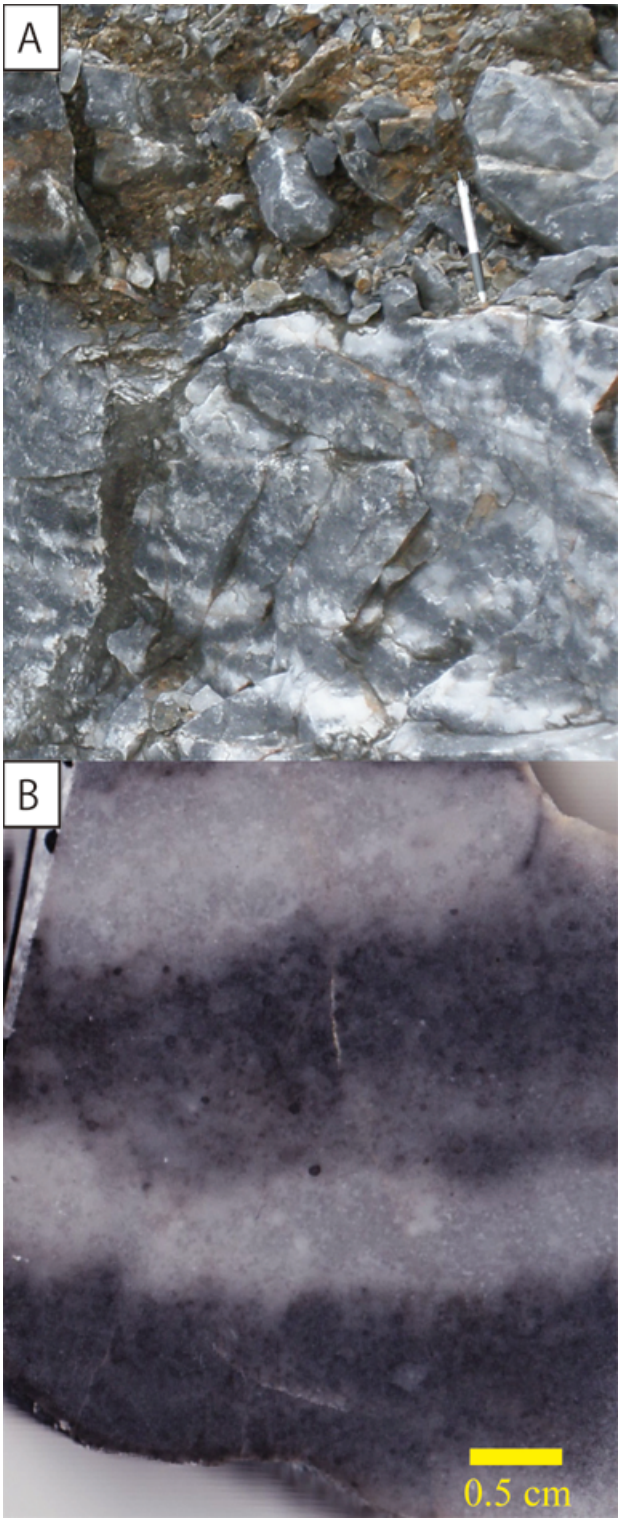

Fig. 4.2. Photograph of outcrop (A) and polished slab (B) of the striped limestone.

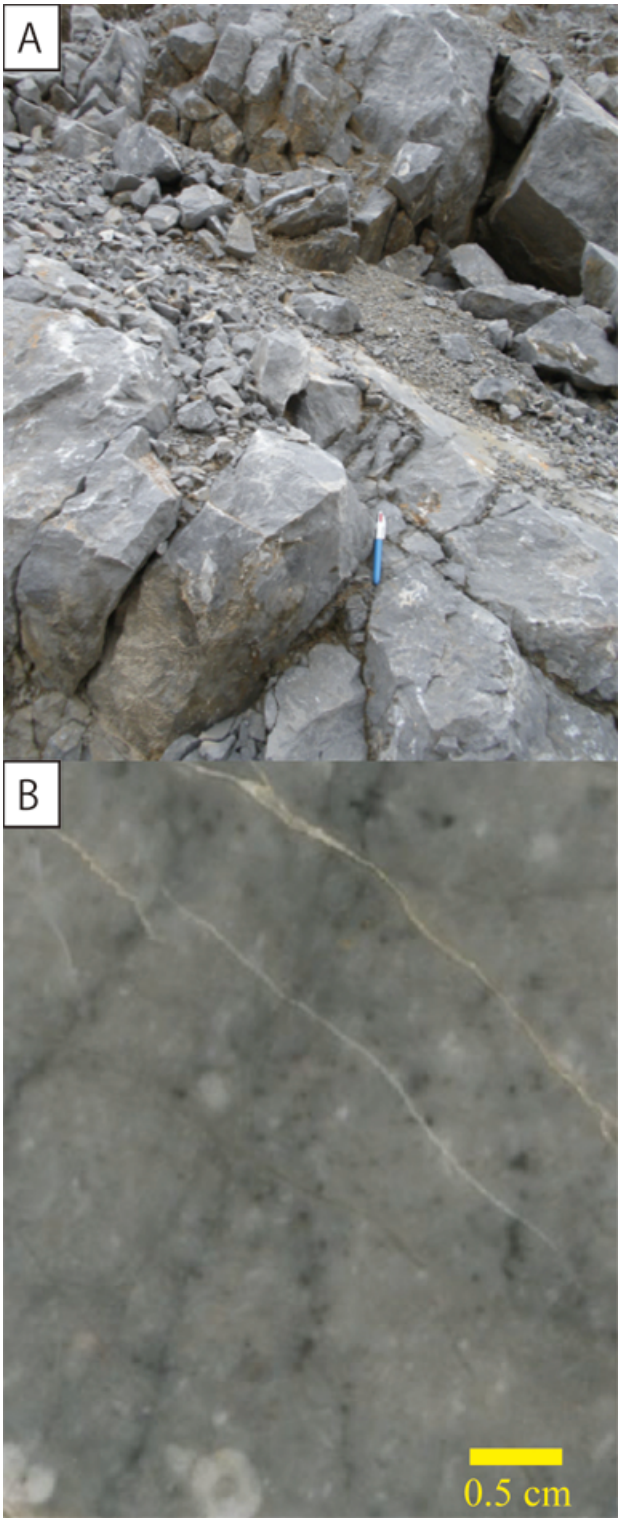

Fig. 4.3. Photograph of outcrop (A) and polished slab (B) of the light gray limestone.

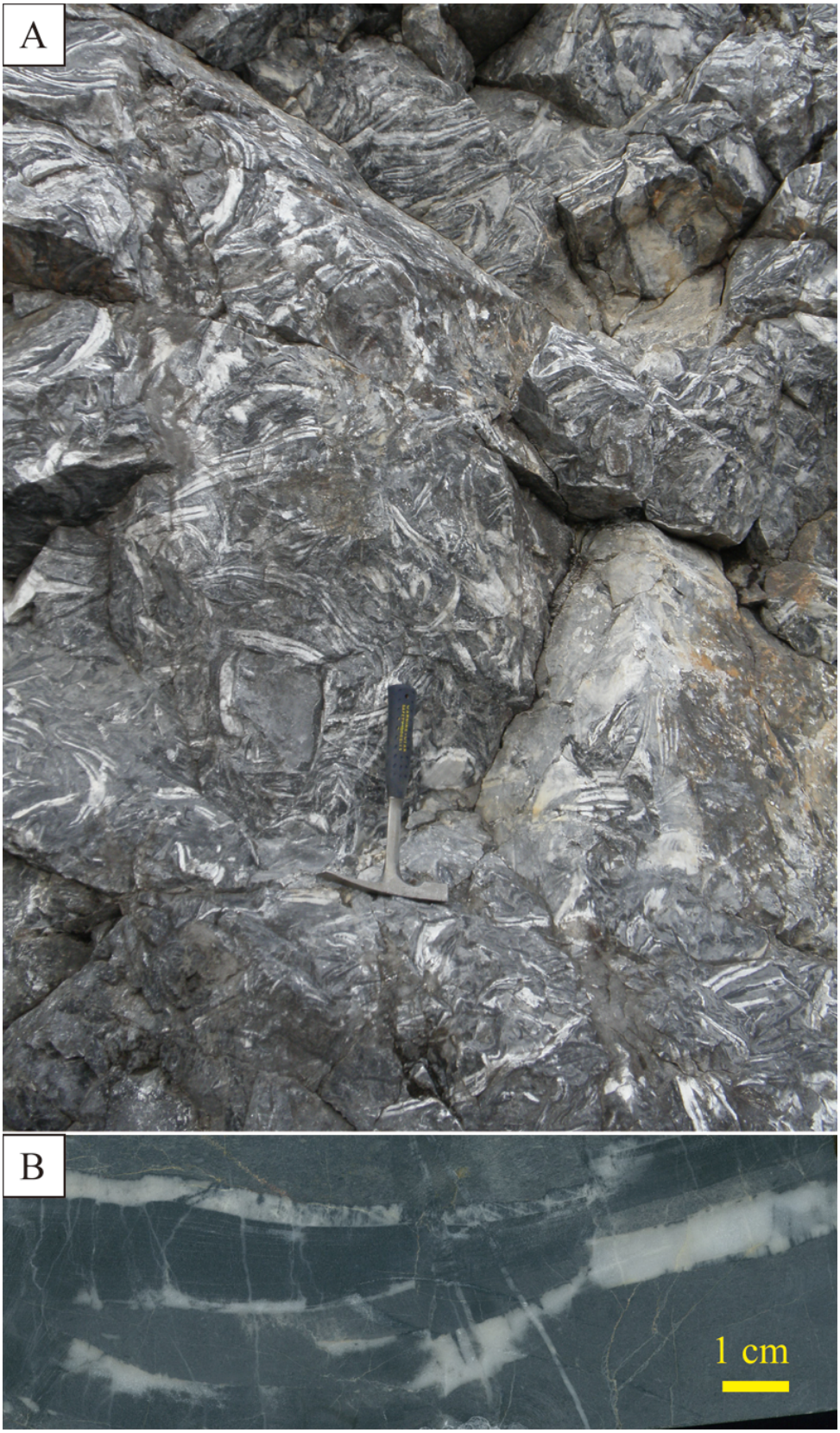

Fig. 4.4. Photograph of large bivalve Alatoconchidae. A) outcrop, B) polished slab. Note that thickness of the shell is more than 2 cm.

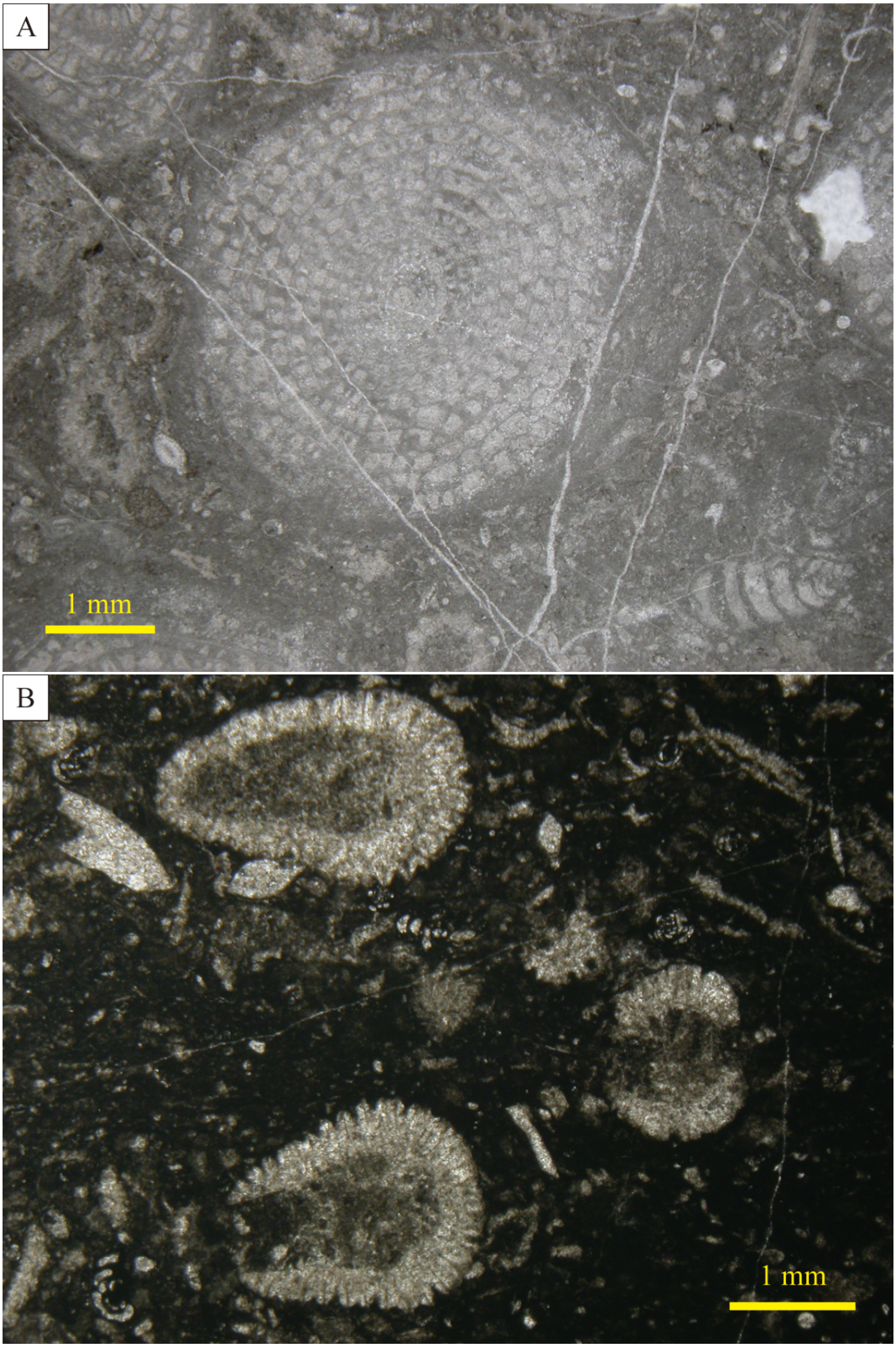

Fig. 4.5. Photomicrographs of the black limestone of subunit B1. A) Fusuline (*Yabeina globosa*) packstone, B) algal (*Mizzia yabei*) wackestone.

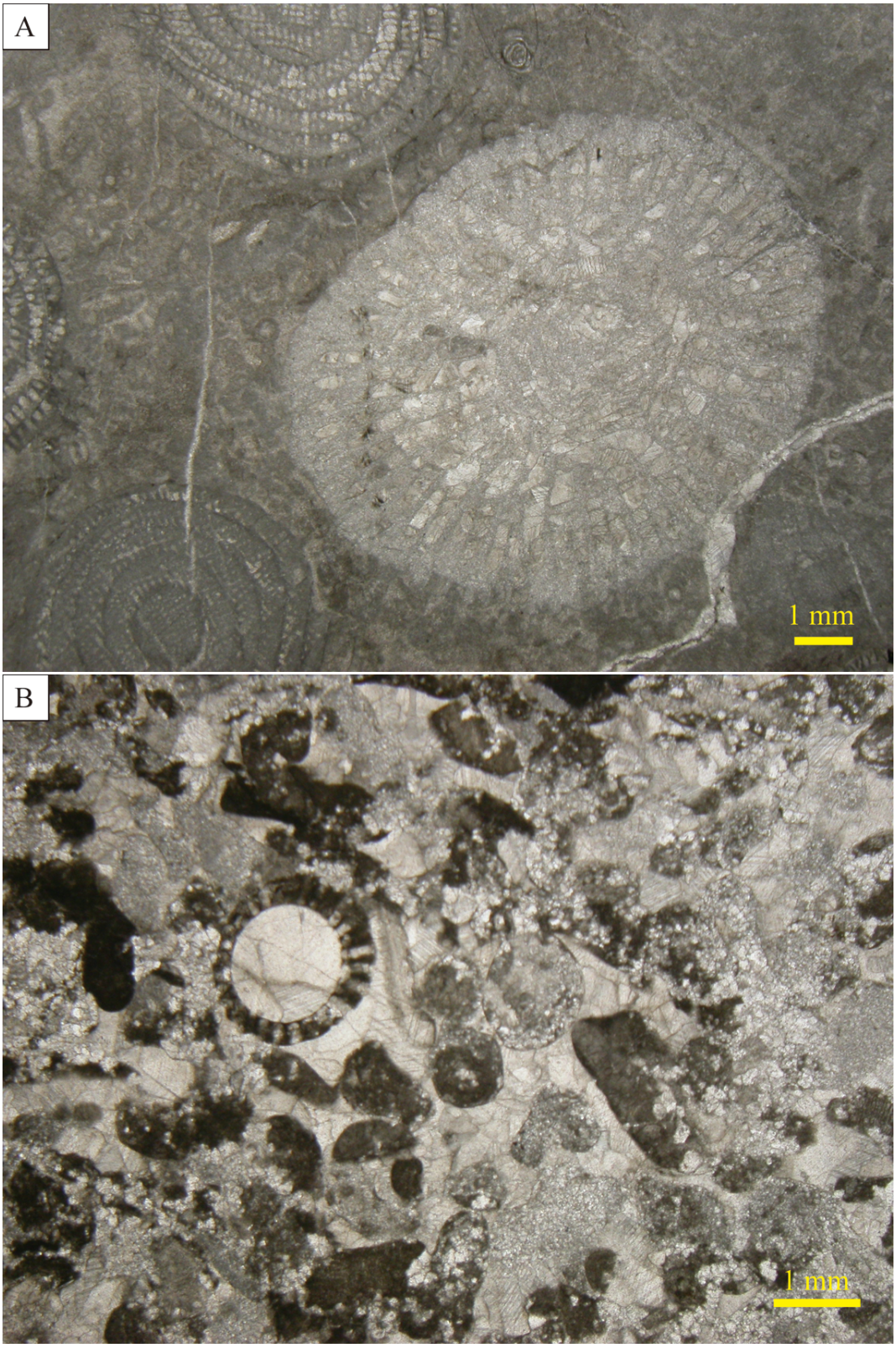
A
1 mm
B
1 mm

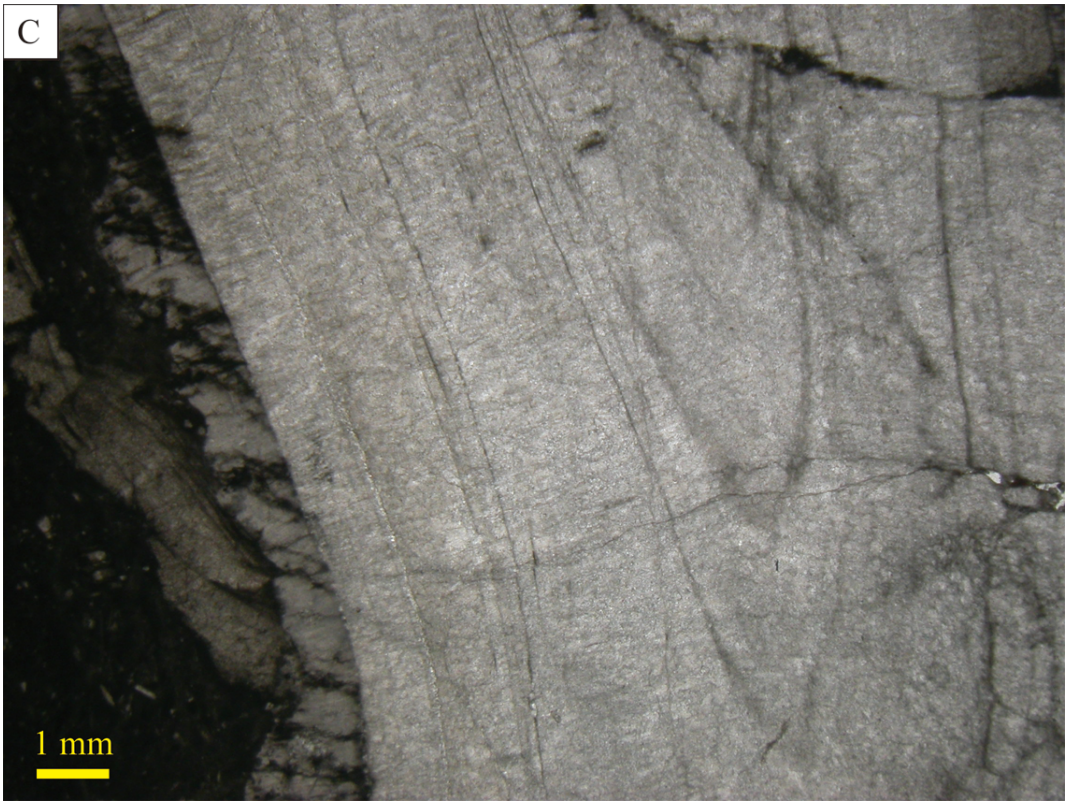

Fig. 4.6. Photomicrographs of the black limestone of subunit B2. A) Coral, fusuline packstone, B) grainstone that lacks lime-mud and consists of sparite. C) Alatoconchidae shell. Typical U-shape shell is observed.

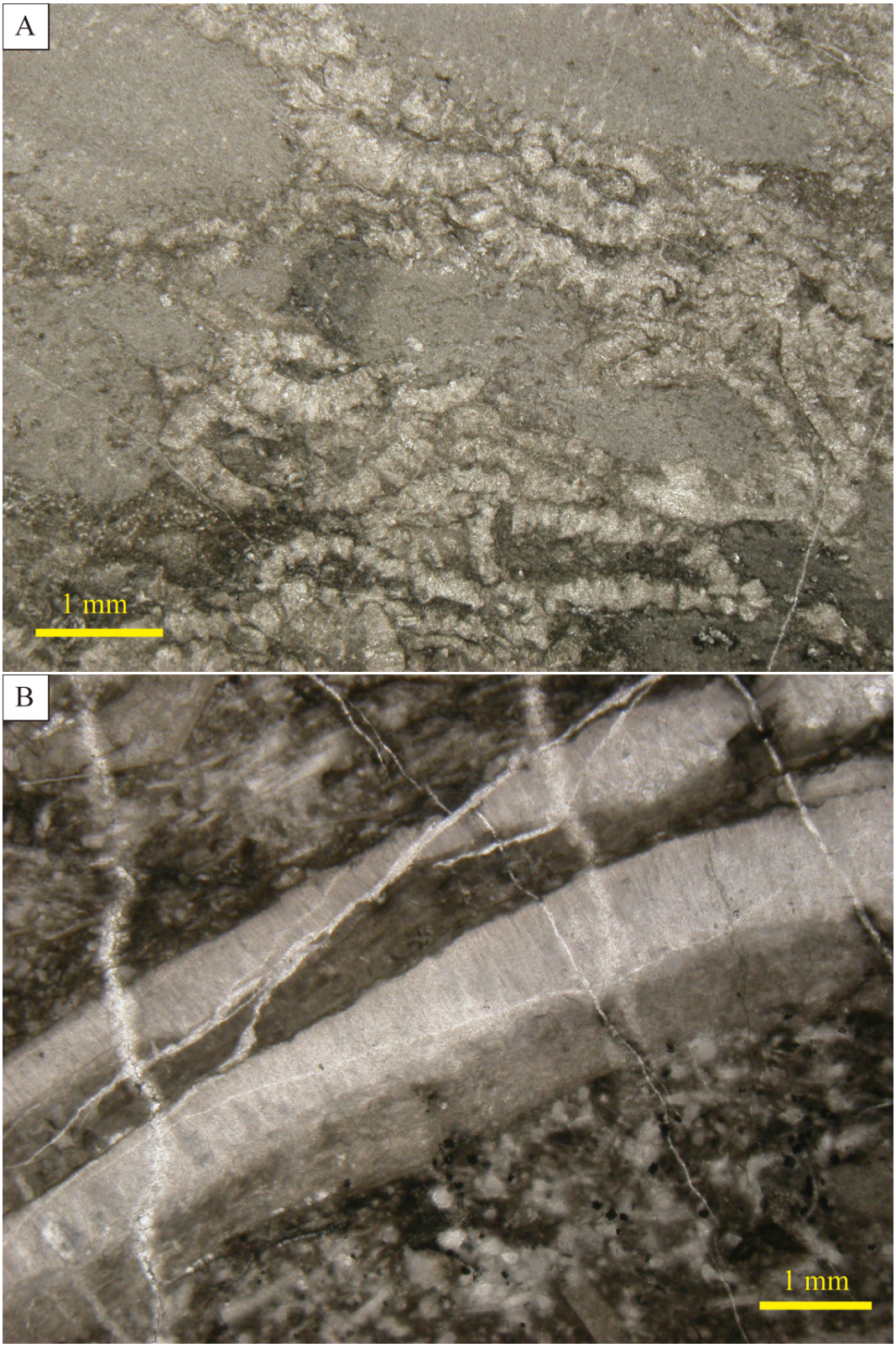

Fig. 4.7. Photomicrographs of the black limestone of subunit B3. A) Algal, fusuline packstone, B) Alatoconchidae prismic and mosaic shell.

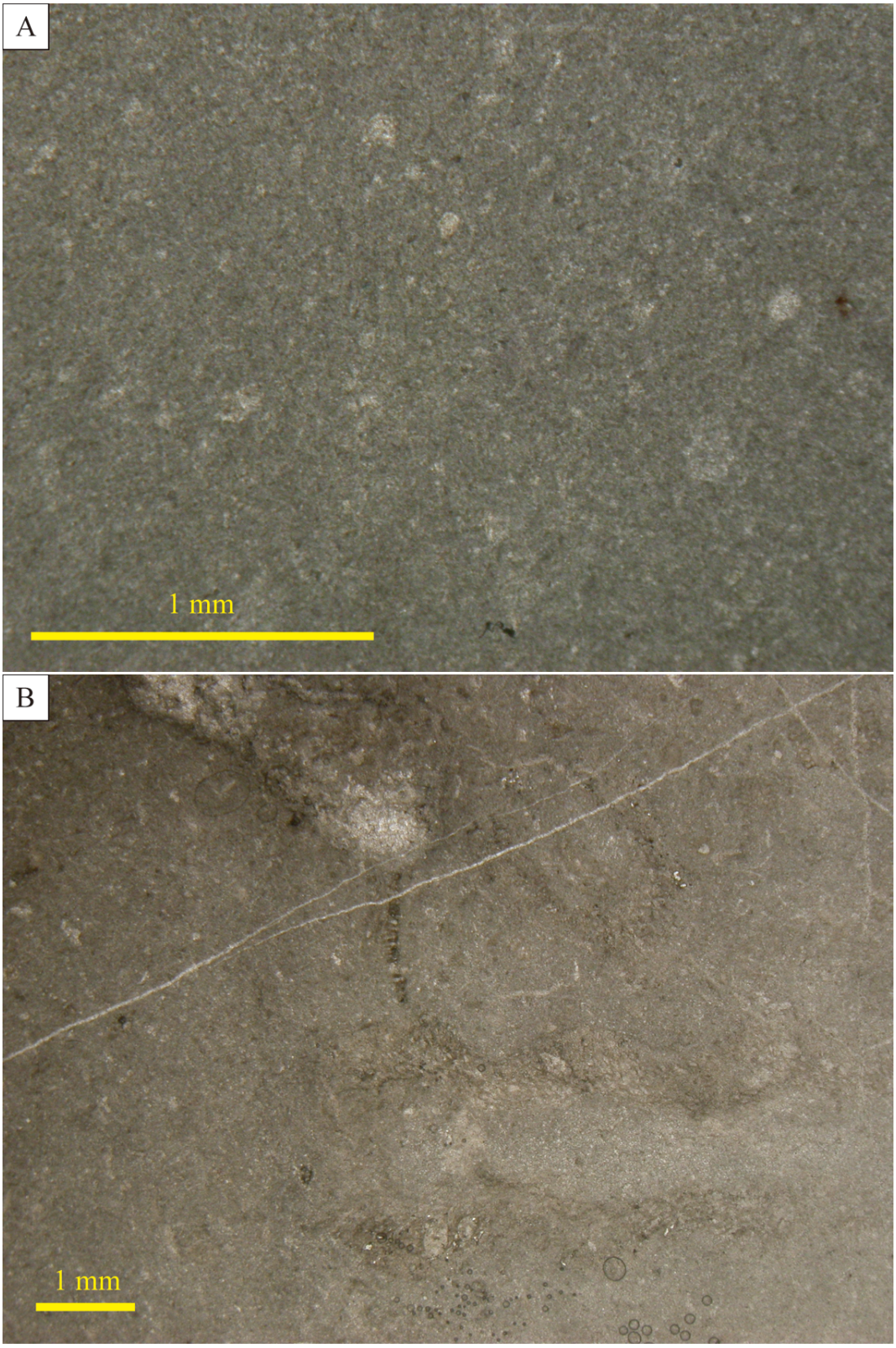

Fig. 4.8. Photomicrographs of the black limestone of subunit B4. A) Fossil-rare wackestone, B) wackestone that yields *Permocalculus* sp.

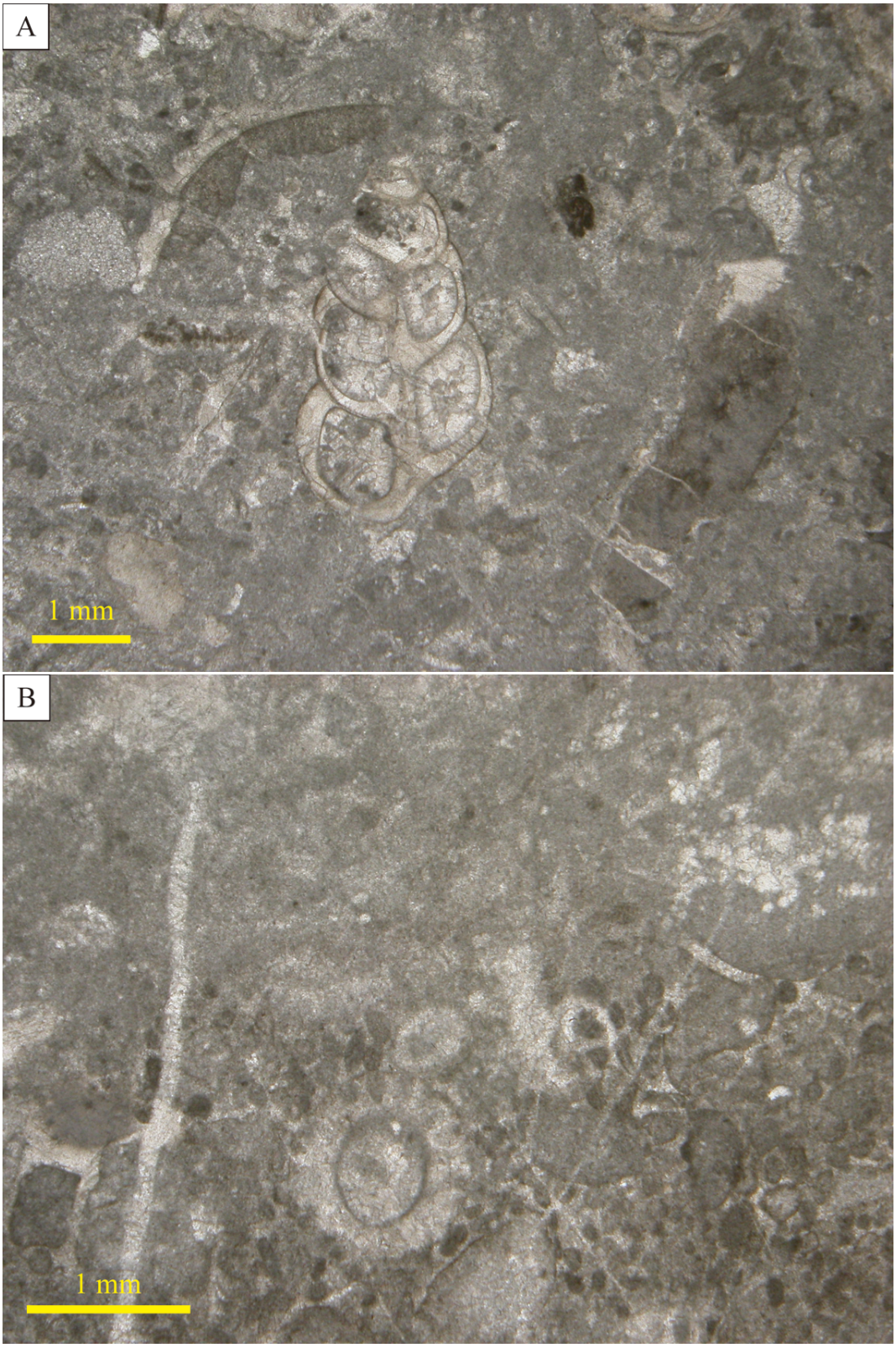
A
1 mm
B
1 mm

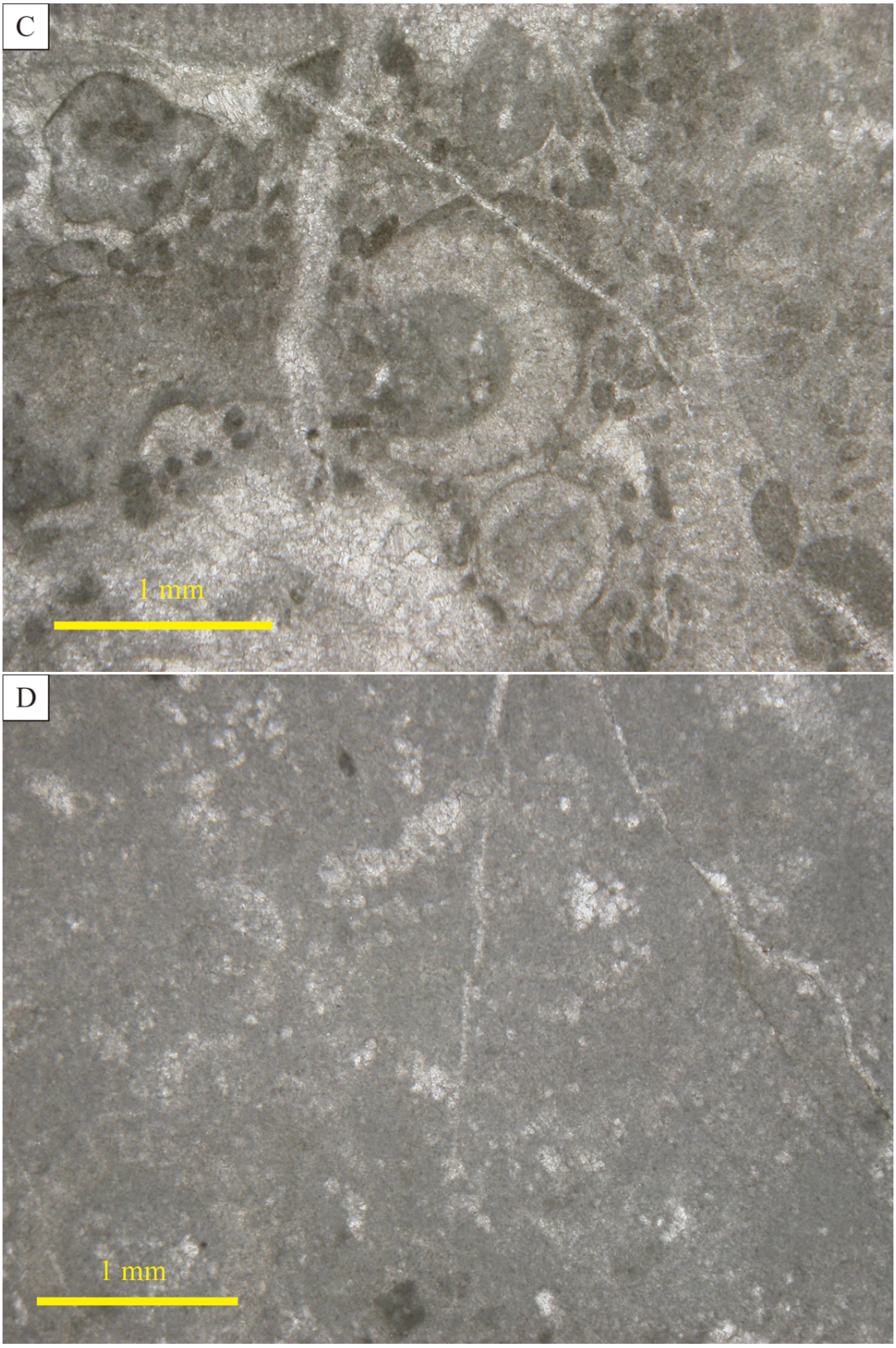

Fig. 4.9. Photomicrographs of the striped limestone of subunit S1. A) Uppermost gastropod in the KW section, B) black-white striped part, C) black part which yields algae and peloids, D) white part which yields rare fossils.

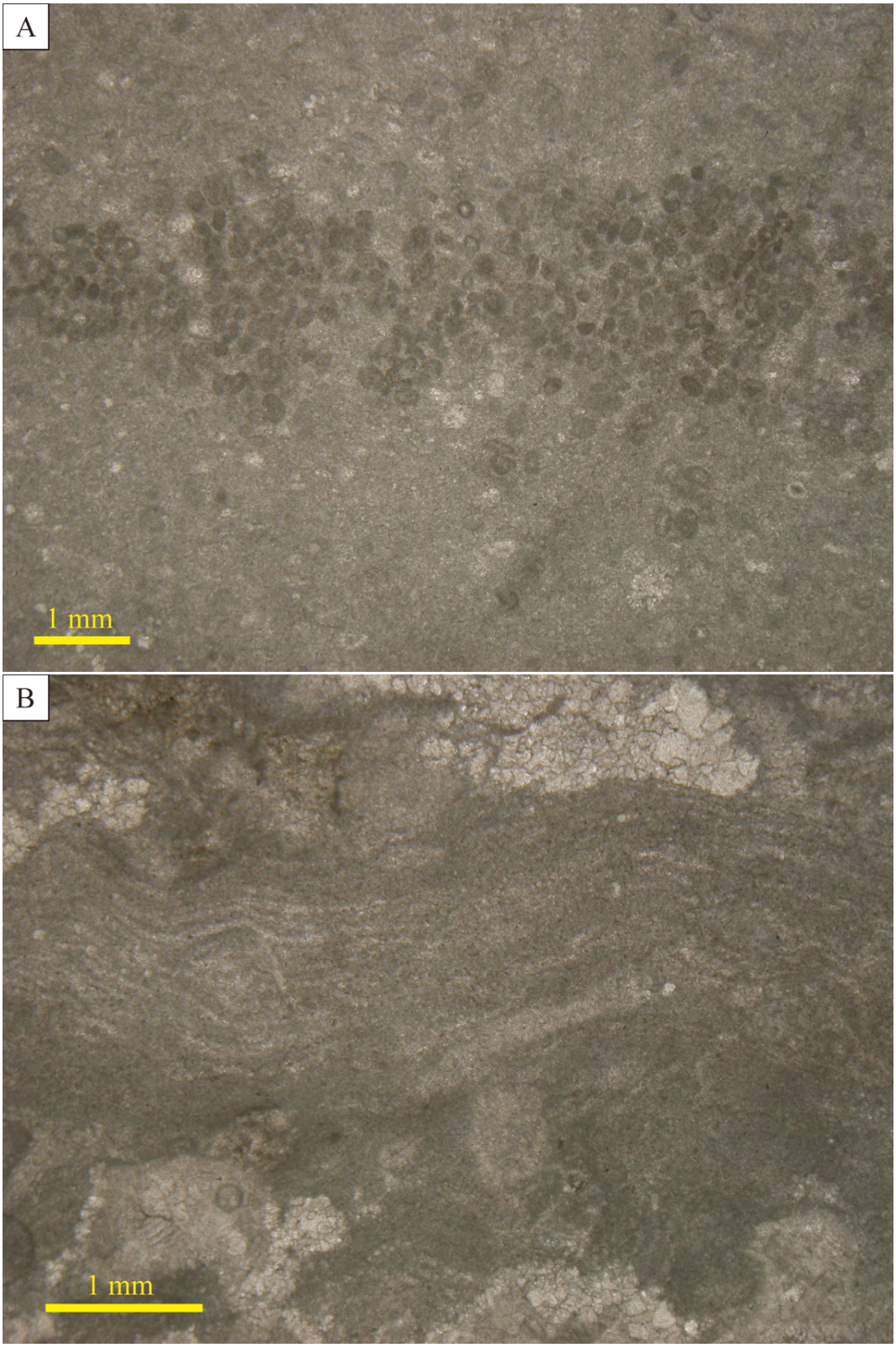

Fig. 4.10. Photomicrographs of the striped limestone of subunit S2. A) wackestone which conisists of peloid-rich black band and peloid-poor gray part, B) sparitic algal wackestone.